Spring 2010

Integration and characterization of an electrical storage system for a hydrogen fuel cell plug-in hybrid electric vehicle

Edward Alexei Anculle Arauco

INTEGRATION AND CHARACTERIZATION OF AN ELECTRICAL STORAGE SYSTEM FOR A HYDROGEN FUEL CELL PLUG-IN HYBRID ELECTRIC VEHICLE

by

EDWARD ALEXEI ANCULLE ARAUCO

A THESIS

Presented to the Faculty of the Graduate School of the

MISSOURI UNIVERSITY OF SCIENCE AND TECHNOLOGY

In Partial Fulfillment of the Requirements for the Degree

MASTER OF SCIENCE IN MECHANICAL ENGINEERING

2010

Approved by

John W. Sheffield
Frank Liou
Scott E. Grasman

ABSTRACT

Hydrogen fuel cell hybrid vehicles are an advance technology that promises to solve the energy crisis in transportation and green houses emissions. Even more, Plug-in or extended range vehicles can add diversity in energy sources. Extended range vehicles have the capability to extract energy from the grid and hence reduce the cost of operation of the vehicle. EcoCAR: the NeXt Challenge is a Noth American competition with seventeen schools participating across North America. Missouri S&T is developing a Fuel Cell Plug-in Hybrid electric vehicle which has a large lithium-ion battery able to store 16 kWh. The fuel cell powertrain is a GM donated fuel cell which includes an electric traction motor and three hydrogen storage cylinders. The proposed electrical storage system consist of five A123 modules which thermal, safety and vibrations requirements. The present work illustrates all the integration process, describes the components of the electrical storage system and presents the cost of integration. The case of the electrical storage system is designed to support 20 g of acceleration for a side and front crash and 8g of acceleration for a rollover crash, the electrical storage system modules are vibration isolated with four vibration isolators per module and a failure analysis is presented. The Missouri S&T prototype is entirely made of aluminum with a total cost of $40,656, the total weight of the system is 322.65 kg which represents an energy/weight ratio of 46.59 Wh/kg.

ACKNOWLEDGMENTS

I would like to thank my advisor and my friend Dr. John W. Sheffield for his help and guidance in my Master degree. He encouraged my development in innumerable ways and I will always be grateful. I would like to thank my professors and committee members Dr. Frank Liou and Dr. Scott Grasman for their help in the success of this work.

I am grateful to the Mechanical and Aerospace Engineering Department at the Missouri University of Science and Technology for supporting this project and supporting the Missouri S&T EcoCAR team.

I would also like to thank the organizers, Frank Falconne, Kristen de la Rosa and Mike Wahlstrom of the EcoCAR: The NeXt challenge for doing this amazing project. My infinite gratitude to our GM mentors Chris Graham, Chris Lawrence and Chris Thomason for their patience and knowledge. A special mention to our sponsors specially A123 Systems and Bachman Machine Company for their support in the develop of the battery system.

Missouri S&T EcoCAR team is a dynamic, dedicated and diverse group of people and between all of them I will always remember my friends Andrew Meintz, Joseph Ishaku, Vijay Mohan, Aanchal Shah and our team leader Kevin Martin. Moreover, I would like to mention my everyday friends and constant support of Michelle, Geonsik and Chrystian.

Finally, this work is dedicated to my parents Huberth and Vilma for the best gift that they could have ever given me: education.

TABLE OF CONTENTS

LIST OF ILLUSTRATIONS

LIST OF TABLES

1. INTRODUCTION

1.1. PROBLEM STATEMENT

Currently, there is considerable interest around the world in the development of new vehicle technologies to reduce greenhouse gas emissions and the dependence upon petroleum. The most promising technology to replace the Internal Combustion Engine (ICE) is the Hydrogen Fuel Cell. Hydrogen is sometimes considered the ultimate clean fuel due to its different renewable pathways from which it can be produced. Table 1.1 describes the architecture of different powertrain components according to Powertrain System Analysis Toolkit (PSAT).

Table 1.1 Powertrain architectures

	Name	**PSAT standard components**	**Mode**	**Fuel**
ICE SI CI	Internal Combustion Engine Vehicle	Starter, engine, mechanical accessories, clutch, gearbox, differential, torque coupling, generator, low voltage battery and electrical accessories.	Full ICE	Gasoline, Diesel, CNG, LNG, H2, E85, LPG, M85, B20.
EV	Electric Vehicle	High voltage power battery, electric motor, gearbox, differential, DC/DC converter and electrical accessories	Full Electric	Electricity

Table 1.1(cont.) Powertrain architectures

HEV	Hybrid Electric Vehicle	Engine, mechanical accessories, torque coupling, generator, high voltage low power battery, DC/DC converter, electric motor, electrical accessories, gearbox, differential.	Electric vehicle mode, cruise mode, overdrive mode, battery charge mode, power boost mode, negative split mode	Gasoline, Diesel, CNG, LNG, H_2, E85, LPG, M85, B20.
PHEV	Plug-in Hybrid Electric Vehicle	Engine, mechanical accessories, torque coupling, generator, high voltage low power battery, DC/DC converter, electric motor, electrical accessories, gearbox, differential and electrical charger.	Charge-depleting, charge sustaining and blended mode.	Electricity, Gasoline, Diesel, CNG, LNG, H_2, E85, LPG, M85, B20.
FEV	Fuel Cell Electric Vehicle	Fuel Cell, DC/DC converter, electric motor, gearbox, differential, Low power battery, electrical accessories.	Electric vehicle mode, cruise mode, overdrive mode, battery charge mode, power boost mode, negative split mode	Hydrogen
FC-PHEV	Fuel Cell Plug-in Hybrid Electric Vehicle	Fuel Cell, DC/DC converter, electric motor, gearbox, differential, high power voltage battery, charger, electrical accessories.	Charge-depleting, charge sustaining and blended mode.	H_2, electricity

In order to ensure the consumer acceptability an extensive analysis must be performed to correctly integrate the different components of the fuel cell hybrid vehicle. Charge depleting hybrid vehicles however have a bigger challenge with the large electrical storage system requirements.

1.2. OBJECTIVES

This work presents the mechanical integration of the several components of an electrical storage system in an extended range fuel cell hybrid vehicle. The work was realized in parallel with the design and integration of the Missouri S&T Fuel Cell Plug-in Hybrid Electric Vehicle (FC-PHEV).

The specific challenge of the Missouri S&T vehicle is to integrate several Fuel Cell Chevy Equinox (GMT101X) fuel cell hybrid components into the Saturn VUE and then turn it into a plug-in vehicle with the large Electrical Storage System (ESS). The ESS main components have been donated from A123®. The GM Saturn VUE 09 is illustrated in Figure 1.1[1].

Figure 1.1. Saturn VUE 2009 [1]

The components of the ESS and devices for the correct operation are extensively described in the present document, furthermore the packaging of the ESS assembly with all the mechanical constraints are analyzed.

1.3. PROBLEM BACKGROUND

Around the world, energy crisis, air pollution and Green House Gases (GHG) emissions due to dependence upon fossil fuels, have generated a big concern and has become a serious problem in human development.

In 2006, most of the world's marketed energy used was produced by liquid fuels followed by coal and natural gas representing almost 88% of the share [2]. This means that most of all the energy used in the world is non-renewable energy. The United States of America follows the same distribution, the petroleum supplies 10.87×10^{12} kWh, natural gas 6.97×10^{12} kWh and coal 6.59×10^{12} kWh. Furthermore, 71% of the total petroleum energy is used for transportation which represents the 95% of the total energy used in transportation [3].Figure 1.2 illustrates the supply sources of energy as well as the demand sectors. Transportation uses almost all energy from petroleum and it represents a large portion of the total energy used in the country. Finally, the depleting of petroleum is causing a significant increase in its price, for example the price of a barrel of petroleum on July 2008 was $135, significantly higher than the price of $30 on January 2003. [4]

The main GHG are water vapor (H_2O), carbon dioxide (CO_2), methane (CH_4), nitrous oxide (N_2O), ozone (O_3) and chlorofluorocarbons (CFC). CFC is an organic compound that contains carbon, chlorine and fluorine. The component that contributes more to the green house effect is the water vapor followed closely by the carbon dioxide. However, carbon dioxide is the component that had grown more in the last century, since the global fossil carbon emissions in 1900 was less than a half of thousand million metric tons of carbon but in 2008 the emissions were 8 thousand million of metric tons. This represents an increase of 1600% [5].

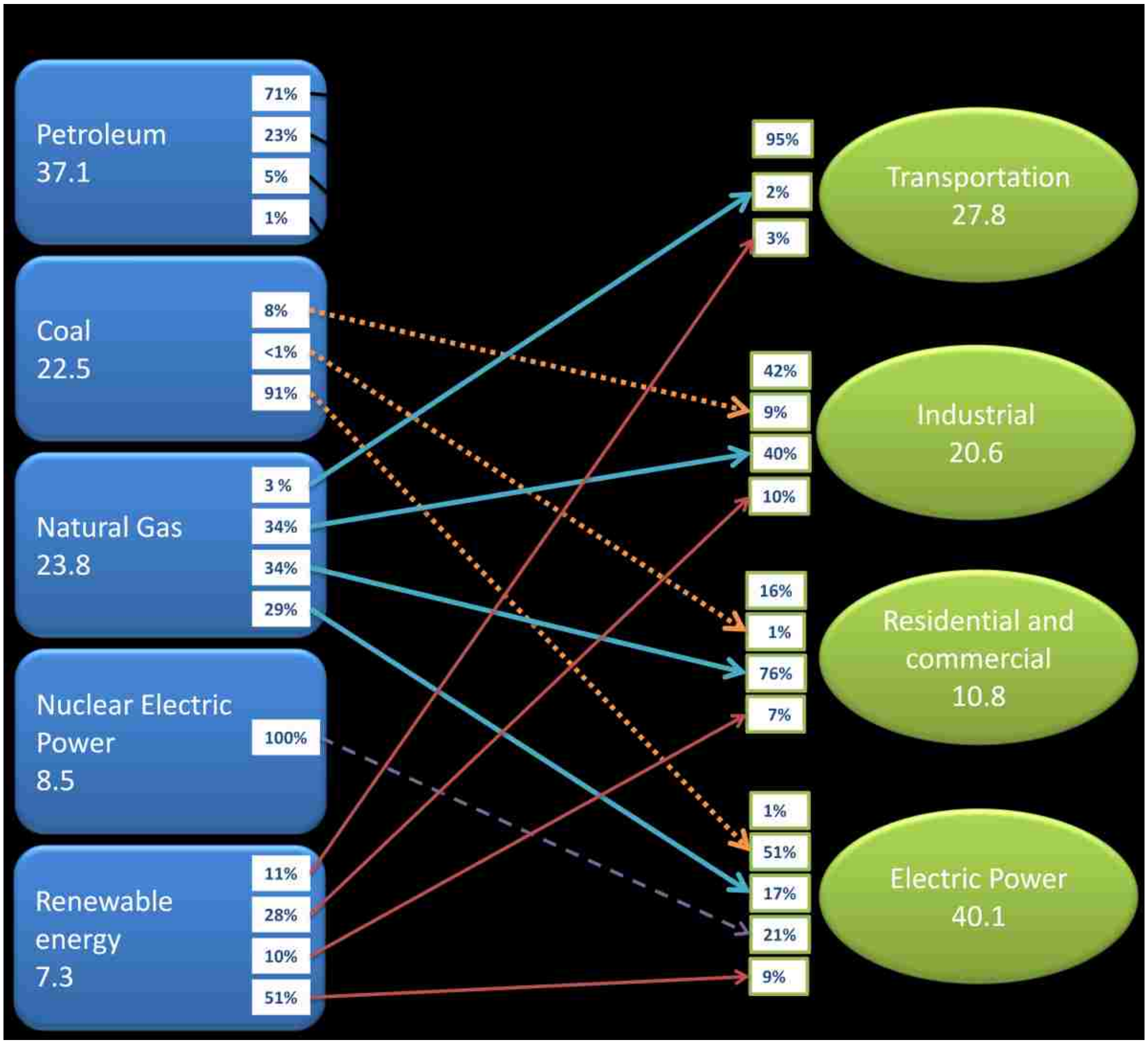

Figure 1.2. Primary Energy Consumption by Source and Sector, 2008 (Quadrillion BTU)

The warming effect on our climate due to increase of GHG, mainly carbon dioxide, is a fact widely accepted in the scientific community [6]. The effects that global warming have on the ecosystem and economy, have been modeled and are predicted to be severe, including increased tropical storms, droughts, and floods [7]. Poor air quality in urban areas caused by vehicle emissions has a significant negative impact on human health [8]. In United States of America, 35% of the transportation greenhouse gas emissions are produced by passenger cars followed by the light trucks with 27%, heavy-duty vehicles with 19% and aircraft with 9%. [9]

The U.S.A's light-duty vehicle fleet consists of approximately 135 million cars and 100 million light-trucks which include pick-ups, minivans and sport utility vehicles (SUVs). New sales in 2006 totaled to nearly 16.6 million units, comprising 81 million passenger cars and 8.5 million light-trucks, or approximately 7 percent of the total LDV fleet [10]. In 20th century the original reason for using petroleum derivates as the main fuel for transportation was the easy extraction, availability and transportation. However, now the demand of this energy source is really large and its proved reserves are mainly in countries with political issues. Moreover, its huge supplies are concentrated in a specific area of the world which creates huge issues in transportation and distribution. For example, while in the United States of America there were 30.5 thousand million of barrels in 2008, in Saudi Arabia there was 264.2 thousand million barrels of oil [11]. This comparison is only in energy, however for extraction purposes, power is an additional constraint for continuously using this source of energy.

In 2008, the production of oil in United States of America was 6736 thousand barrels daily, which means the 7.8% of the total share; this production is more than most of the Middle East countries production [12]. Figure 1.3 illustrates the proved reserves of oil used in the world.

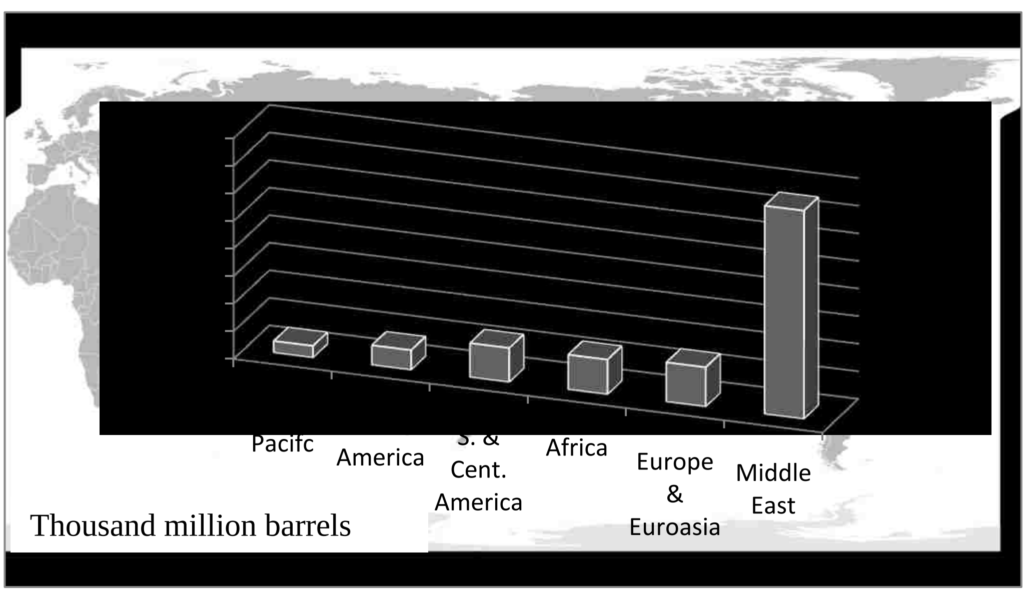

Figure 1.3. Proved reserves of oil in 2008

1.4. PLUG-IN HYBRID VEHICLE POWERTRAINS

The Institute of Electrical and Electronics Engineers (IEEE) defines Plug-in Hybrid Electric Vehicles PHEV as a car, truck or other vehicle that can be driven solely by an electric motor for at least ten miles without consuming any gasoline (called a "PHEV-10"), and with batteries that can be recharged by plugging it into a wall outlet. [13]

The PHEV has several advantages over regular vehicles. It has better fuel efficiency, significantly reduces the GHG, reduces operating costs, better mileage than all electric vehicles, reduces smog and has the plug-in capability which improves the use of electricity.

PHEVs are considered more energy efficient vehicles because they can be charged during off peak periods, and are equipped with technology to shut off charging during periods of peak demand. Finally, extended range vehicles have the ability to load balance and help the grid during the peak loads. This is accomplished with the vehicle to grid technology (V2G) By using excess battery capacity to send power back into the grid and then recharging during off peak times using cheaper power, such vehicles are actually advantageous to utilities as well as their owners.

Even if such vehicles just led to an increase in the use of night time electricity they would even out electricity demand which is typically higher in the day time, and provide a greater return on capital for electricity infrastructure [14].

There are several companies already using the technology of PHEVs, for example GM's Chevrolet Volt which is expected to be launched in November 2010. It is a compact car which uses GM Voltec technology. Voltec technology, former E-Flex, is a plug-in powertrain with battery-dominant series hybrid architecture. The main components of the Chevy Volt are: a 1.4l 4-cylinder engine, an electric motor 111 kW peak power output, 16 kWh Lithium-ion battery. It is important to note that the location of the lithium-ion batteries is in the center of the vehicle with a T-shape. The Volt concept and its top view are illustrated in Figure 1.4. [15] [16].

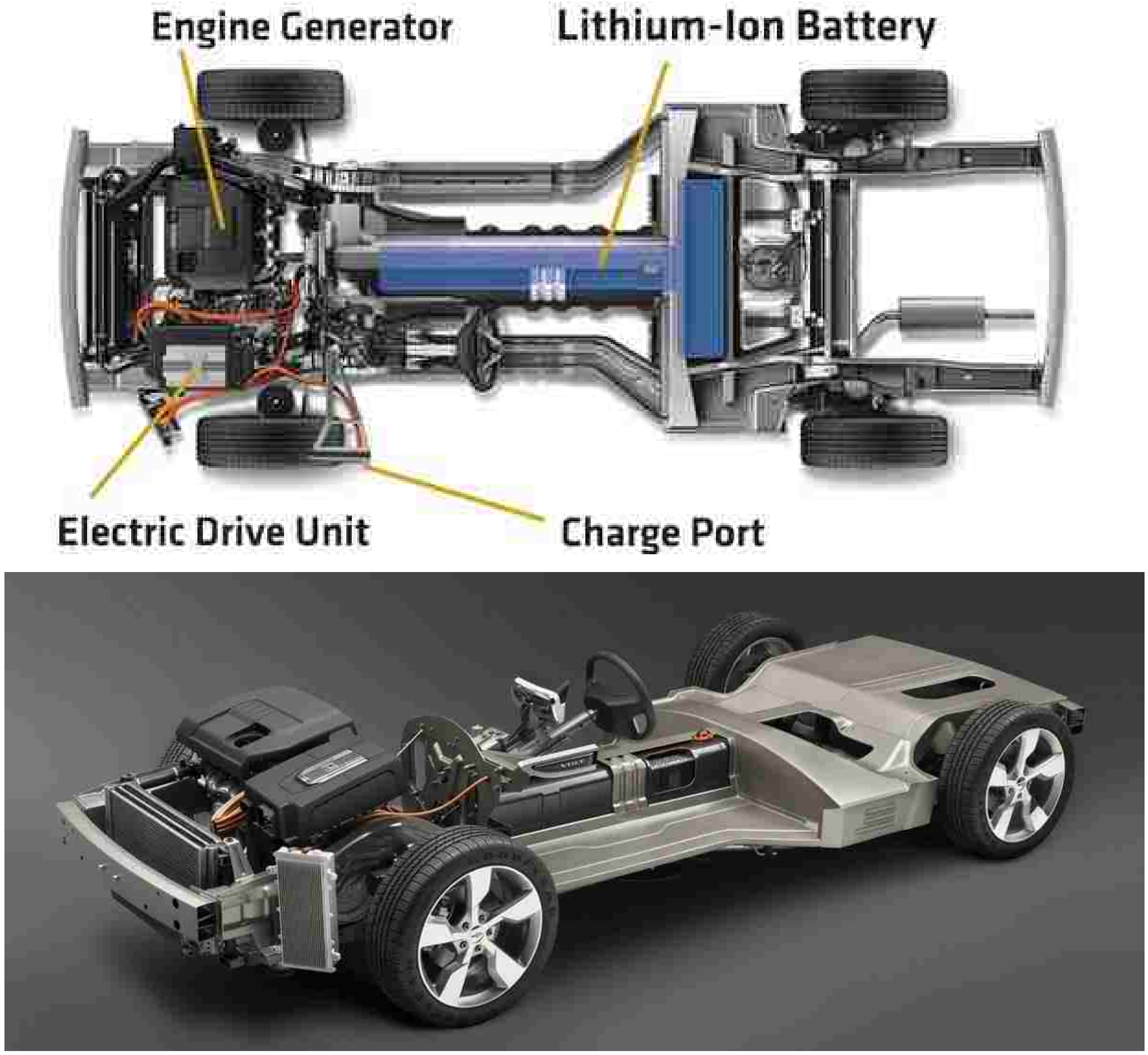

Figure 1.4. GM Chevrolet Volt [15] [16]

Finally, in plug-in vehicle there is a new system that strongly influences the performance of the powertrain. The hybrid vehicles for example, have more than two electrical systems, electrical compressor for the HVAC and more than one loop of cooling system. In addition to all this, the PHEV needs to add a HV charger and a cooling system for large batteries, some of the PHEVs have air cooled system, such as the Chevy Volt, but others use liquid cooled batteries.

1.4.1. Parallel PHEV. In the parallel hybrid vehicle configuration, both the electric motor and the internal combustion engine drive the wheels according to the most optional point and increase the efficiency of the powertrain. There are several configurations to mechanical integration of a parallel PHEV powertrain. Two options for a Front Wheel Drive (FWD) vehicle are illustrated in Figure 1.5. The parallel PHEV is classified as an approach in which the sources of power mechanical are coupled. The top part of the Figure 1.5 illustrates a vehicle where the mechanical interface between the motor and the ICE is differential. Another configuration is showed in the second part of the Figure 1.5 where ICE is directly coupled to the wheels and has a transmotor around the shaft. The parallel configuration in general allows the motor to assist the engine on hard acceleration, as well as to take over completely during low driving speed. This characteristic allows the PHEV to install a small ICE. Moreover, when the car is braking and the State of Charge (SOC) of battery is low, the electric machine operates as a generator to power the battery. Unfortunately, this configuration does not allow the ICE to operate most efficiently.

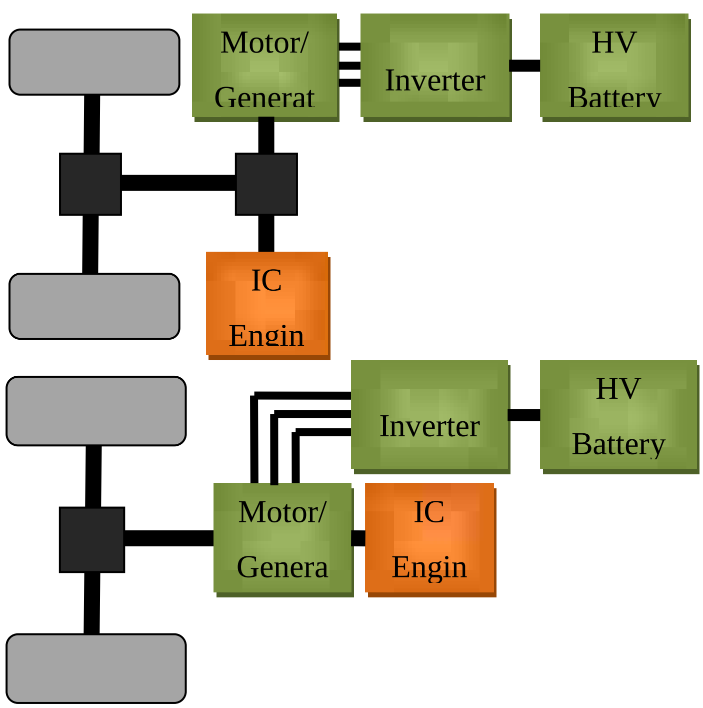

Figure 1.5. Parallel hybrid vehicle configuration

1.4.2. Series PHEV. In the series hybrid vehicle configuration, the internal combustion engine is designed to charge the batteries using a generator. Unlike parallel configuration there is no mechanical interface between the electric machine and ICE. Figure 1.6 illustrates a series configuration.

When the state of charge of the battery reaches its minimum level, the internal combustion engine starts to charge the battery using the generator. When the battery is full, ICE shuts off. The ICEs always run most efficiently in parallel powertrain. Unfortunately, there is still considerable energy lost during the transformation from mechanical energy to electrical energy.

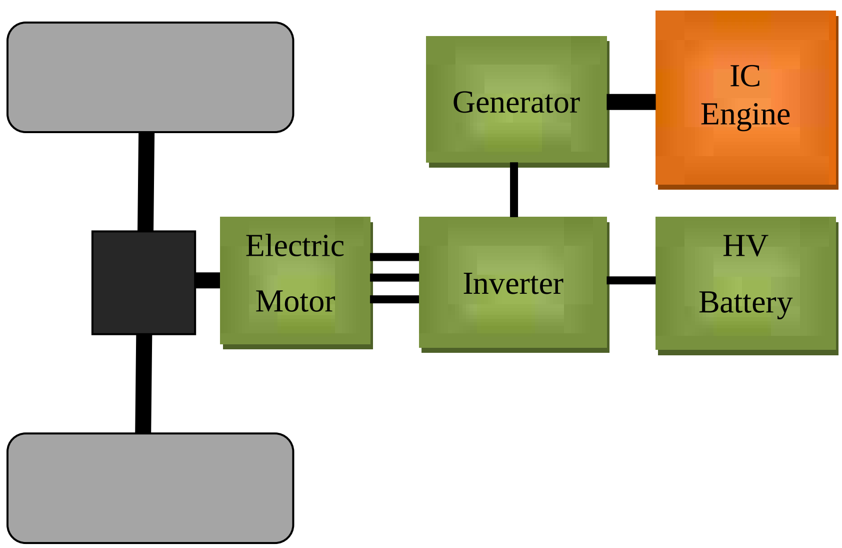

Figure 1.6. Series hybrid vehicle configuration

1.5. TRANSPORTATION HYDROGEN FUEL CELL TECHNOLOGY

Hydrogen is sometimes considered the ultimate fuel due to its different pathways through which it can be produced. Moreover Fuel Cell technology is not new, NASA has used for many years to provide power to space shuttles electrical systems.

PEM Fuel Cell is an electrochemical device that converts hydrogen fuel into energy and water without combustion. Electrodes present on either side of the Proton Exchange Membrane are responsible for carrying electric current. An electrolyte between the electrodes carries the hydrogen ions while not letting the electrons through. PEM fuel cell has fast start up, low sensitivity to orientation and favorable power to weight ratio. These characteristics make this type of fuel cell suitable for passenger vehicles. Finally, most hydrogen fuel cells do not produce enough voltage to power a car so fuel cells are typically arranged in "stacks." The chemistry of a Fuel Cell is presented in Figure 1.7.

.

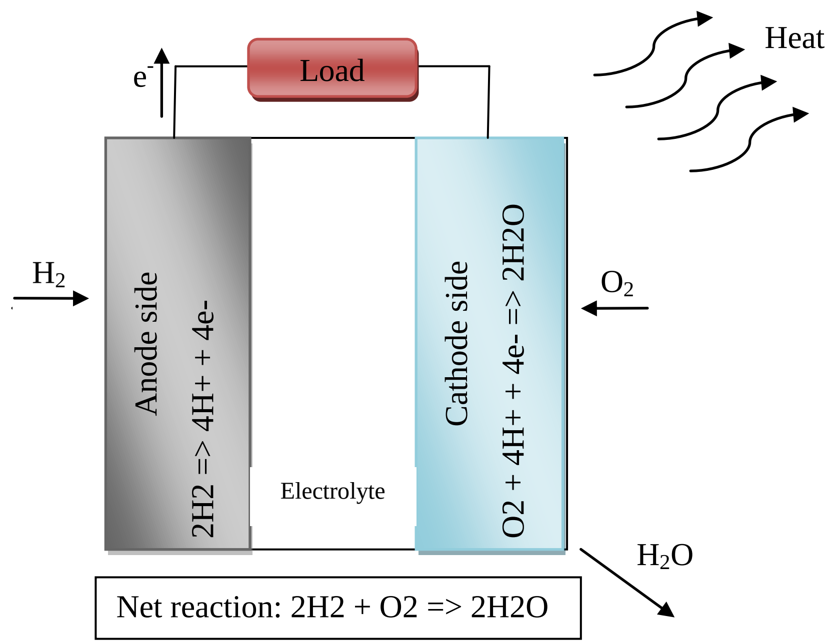

Figure 1.7. Fuel Cell chemical reaction

Several car companies have already started development of the Polymer Electrode Membrane (PEM) fuel cell technology with an exhaustive research in this area, for example General Motors has the Chevy Equinox, a hydrogen fuel cell electric vehicle that can replace a regular SUV in the current market.

The Chevrolet Equinox Fuel Cell is a 5-door front wheel driven SUV with four passenger seats, a cargo volume of 906.24 liters and a payload of 340 kg. The fuel storage system consists of three carbon fiber cylinders storing 4.2 kg of compressed hydrogen gas at 700 bars. The Fuel cell system is able to provide a peak power of 93 kW to the Electrical Traction System. The ETS is a 3-phase asynchronous electric motor with 73 kW continuous, 94 kW maximum power and able to provide 320 Nm of torque. The Battery system is a nickel metal hydride battery pack with regenerative braking and able to provide a peak power of 35 kW. The main components of the FC Equinox are illustrated in Figure 1.8 [18].

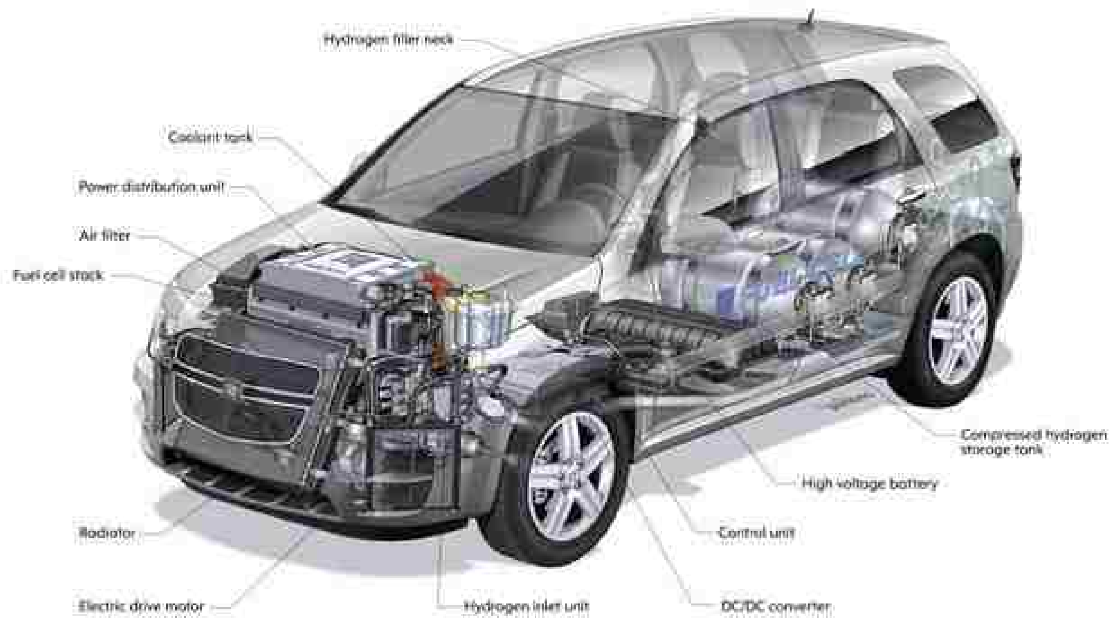

Figure 1.8. Chevy Fuel Cell Equinox [18]

The Fuel cell propulsion system has an operating life of 2.5 years or 80,000 km and its operating temperature is -25^{o}C to +45^{o}C. In addition, the FC Equinox is expected to meet all applicable 2007 U.S. Federal Motor Vehicle Safety Standards (FMVSS). Finally, the Chevy Equinox does not have petroleum consumption; it is an EPA-certified zero-emission vehicle (ZEV) that emits only water vapor. It has a zero propulsion system (greenhouse gases-GHG) emissions and has instantaneous torque [17].

Furthermore, the state of art of the fuel cell vehicles is presented in Table 1.2 [19]. As it can be seen all the important automotive companies around the world had already started the development of this zero emissions powertrain.

Table 1.2. The state of the art of fuel cell vehicle technology [19]

Manufacturer	Vehicle	Hybrid Features
DaimlerChrysler	Modified Mercedes-Benz A-Class "F-Cell"	65 kW drive motor, 350 bar storage, 150 km range
Ford Motor	Modified Ford Focus "FCV"	85 kW fuel cell, NiMH battery, 300 km range
General Motors	Modified Chevrolet Equinox "Equinox Fuel Cell"	93 kW fuel cell, 35kW NiMH battery, 320 km range
Honda	Custom Honda "FCX"	80 kW drive motors, ultra capacitors, 430 km range
Hyundai	Modified Hyundai Tucson "FCEV"	80 kW drive motors, NiMH battery, 300 km range
Nissan	Modified Nissan X-TRAIL "FCV"	85 kW drive motors, Lion battery, 350 km range
Toyota	Modified Toyota Highlander "FCV"	82 kW drive motors, NiMH battery, 330 km range

The conclusion is fuel cell hybrid electric vehicles technologies are in an advanced stage. However, there are still several obstacles which include technical and political issues. Moreover, the hydrogen storage systems for the vehicle range and fuel cell stack mass production are the topics on research and development.

1.6. ADVANCE ELECTRICAL STORAGE SYSTEM

The success of hybrid vehicles technology is primarily due to energy storage systems. There are several energy storage systems that can be applied for the PHEV, which includes ultra capacitors, flow batteries, Ni-Cd batteries, Ni-H_2 batteries and recently lithium ion batteries. Li-ion offer potential advantages in energy density, high discharge voltage, high efficiency of charge/discharge and power density [20] [21].

Moreover, ultra capacitors represent a reliable alternative for FC-PHEV. Simulations indicate that fuel-efficient hybrid-electric vehicles can be designed using either batteries or ultra capacitors and that the decision between the two technologies is dependent on their cost and useful life [22]. Some of the disadvantages of the ultra capacitors are low energy density compared with Li-ion batteries, low working voltage and variable voltage which leads to a more complex power electronics. In a FC-PHEV where the powertrain has large and heavy components the use of ultra-capacitor would increase the weight of the vehicle.

A Lithium-ion battery is a type of rechargeable battery in which lithium ions move from the anode to cathode during discharge, and from the cathode to the anode when charged. Different types of lithium-ion batteries use different chemistry and have different performance, cost, and safety characteristics. Unlike primary lithium batteries, lithium-ion cells use an intercalated lithium compound as the electrode material instead of metallic lithium [23]. The technical characteristics of the current Li-ion battery technology are energy/weight 100-160 Wh/kg, energy/size 250-360 Wh/l, power/weight 250-340 W/kg and charge/discharge efficiency 80-90%.

As a chemical device, lithium-ion batteries can ignite when are exposed to high-temperature or have a short circuiting. For this reason they normally contain safety devices that protect the cells from abuse and to protect users.

A123 System is a leading company on lithium-ion batteries for hybrid and plug-in hybrid vehicles. They offer several types of lithium-ion cylindrical and prismatic configuration such as 18650 cells, 26650 cells, 32113 cells and 20Ah prismatic cells. Figure 1.9 [24] [25] illustrates an A123 prismatic cell assembled in a cell which is a basic component for extended range vehicles electrical storage systems.

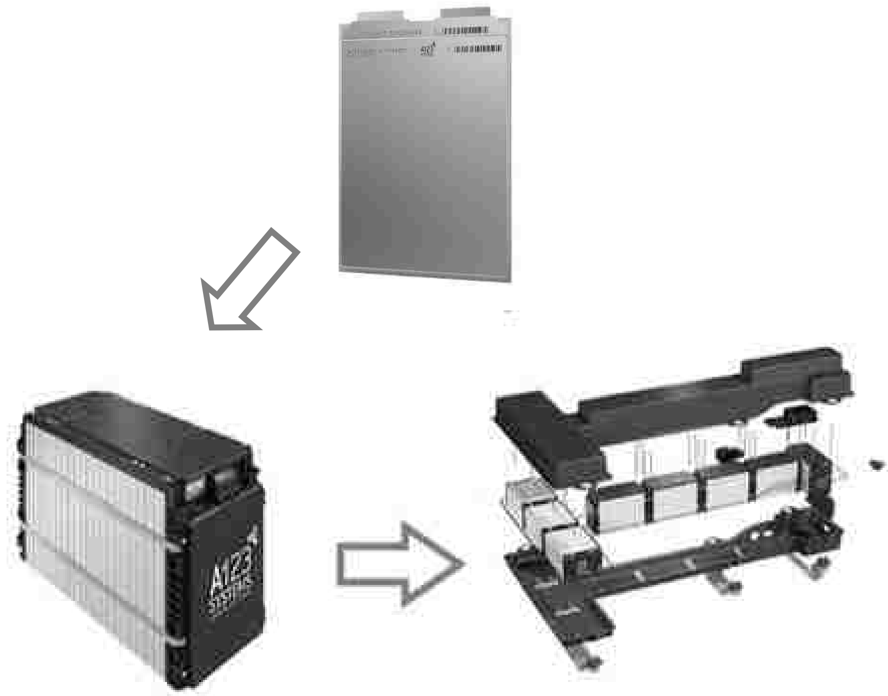

Figure 1.9. Lithium-ion prismatic batteries for plug-in vehicles [24] [25]

2. FUEL CELL PLUG-IN HYBRID ELECTRIC VEHICLE

2.1. ECOCAR: THE NEXT CHALLENGE

This thesis is integrated in parallel with the development of the Fuel Cell Plug-in Hybrid Electric Vehicle (FC-PHEV) in Missouri University of Science and Technology during the periods of 2008-2010. Missouri S&T was selected from over 300 schools to be part of the EcoCAR: The NeXt Challenge.

EcoCAR: The NeXt Challenge is a new collegiate Advanced Vehicle Technology Competition (AVTC) which kicked off in the fall of 2008. Sponsored by the U.S. Department of Energy (DOE) and General Motors (GM), as well as by Natural Resources Canada and other industry leaders, EcoCAR challenges engineering students from universities across North America to re-engineer a GM vehicle, minimizing energy consumption, emissions, and greenhouse gases while maintaining the vehicle's utility, safety, and performance[26].

The challenge selected 17 schools across United States of America and Canada, between all of them only two schools were selected to receive a hydrogen system to integrate it into the school's powertrain, Missouri S&T from United States of America and Waterloo from Canada.

During the first year of EcoCAR competition, the teams used math based design tools such as Powertrain Systems Analysis Toolkit (PSAT) in order to select an advanced vehicle powertrain to meet the technical specifications of the competition. Moreover, teams used CAD software to ensure that their chosen components fit into their donated vehicle and that the electrical, mechanical and software systems function properly. Finally, teams also used software-in-the-loop (SIL) and hardware-in-the-loop (HIL) to develop better controls and subsystems.

The Finals of the first year was in Toronto Canada in summer 2009, it was an entire week full of presentations, reports and several types of events Figure 2.1 [27] illustrates all the members of EcoCAR: The NeXt challenge that includes team members, sponsors and organizers.

Figure 2.1. EcoCAR: The Next Challenge first year finals [27]

The second year of EcoCAR competition is focused on the mechanical integration of the different components selected in the previous year. In November 2009, Missouri S&T received a Saturn VUE 2009 which is a mid-size SUV with a unibody structure construction.

Finally, the team is using NX Siemens® for the CAD integration and most of the finite element analysis was perform with ANSYS® and FLUENT®.

2.2. VEHICLE ARCHITECTURE DESCRIPTION

Missouri S&T EcoCAR team performed several simulations of the Powertrain System Analysis Toolkit (PSAT) in the first part of the design in order to determine the best architecture for the competition. After several simulations the team decided to integrate a Fuel Cell Plug-in Hybrid Electric Vehicle (FC-PHEV) and its characteristics are presented in the Vehicle Technical Specification in Table 2.1[28].

The teams vehicle technical specification (VTS) has to achieve the competition requirements, which are defined mainly by the production VUE 09 specifications. The range does not achieve the competition requirements and the weight is in the limit allowed. During the mechanical integration these parameters are considered to keep the vehicle in the competition requirements.

Table 2.1. Missouri S&T EcoCAR vehicle technical specifications

Specification	**Competition**		**Missouri S&T VTS**
EcoCAR	Production VUE	Competition Requirement	VTS
Acceleration from 0 to 60	10.6 s	≤ 14 s	9.8
Acceleration from 50 to 70	7 s	≤ 10 s	5.8
UF Weighted FE *	8.3 l/100 km	7.4 l/100 km	7.4 l/100 km
Towing Capacity	680 kg (1500 lb)	≥ 680 kg @ 3.5%, 20 min @ 72 kph	680 kg @45 mph
Cargo Capacity	0.83 m^3	Height: 457 mm Depth: 686 mm Width: 762 mm	0 .83 m3
Passenger Capacity	5	≥ 4	4
Braking 60 - 0	38 m- 43 m	< 51.8 m	< 51.8 m
Mass	1758 kg	≤ 2268 kg	2238 kg
Starting Time	≤ 2 s	≤ 15 s	≤ 15 s
Ground Clearance	198 mm	≥178 mm	≥178 mm
Range	> 580 km	≥ 320 km	305 km

The powertrain of the proposed architecture consists of a GM proprietary 95 kW PEM hydrogen fuel cell, A123® Systems 16 kWh Lithium-ion prismatic modules, BRUSA® DC/DC converter, MOTOTRON® controller and an 80 kW continuous 110 kW peak power electric motor which are connected in series architecture. Figure 2.2 shows the main components and location of the of Missouri S&T architecture.

This FC-PHEV achieves a plug-in hybrid characteristic for the vehicle with a large 16 kWh electrical storage system and the BRUSA NLG5 charger. The ESS system consists of five series connected modules which have several sub-system requirements, such as specific temperature, safety exhaust system and vibration requirements. All these systems will be discussed and presented in the following chapters.

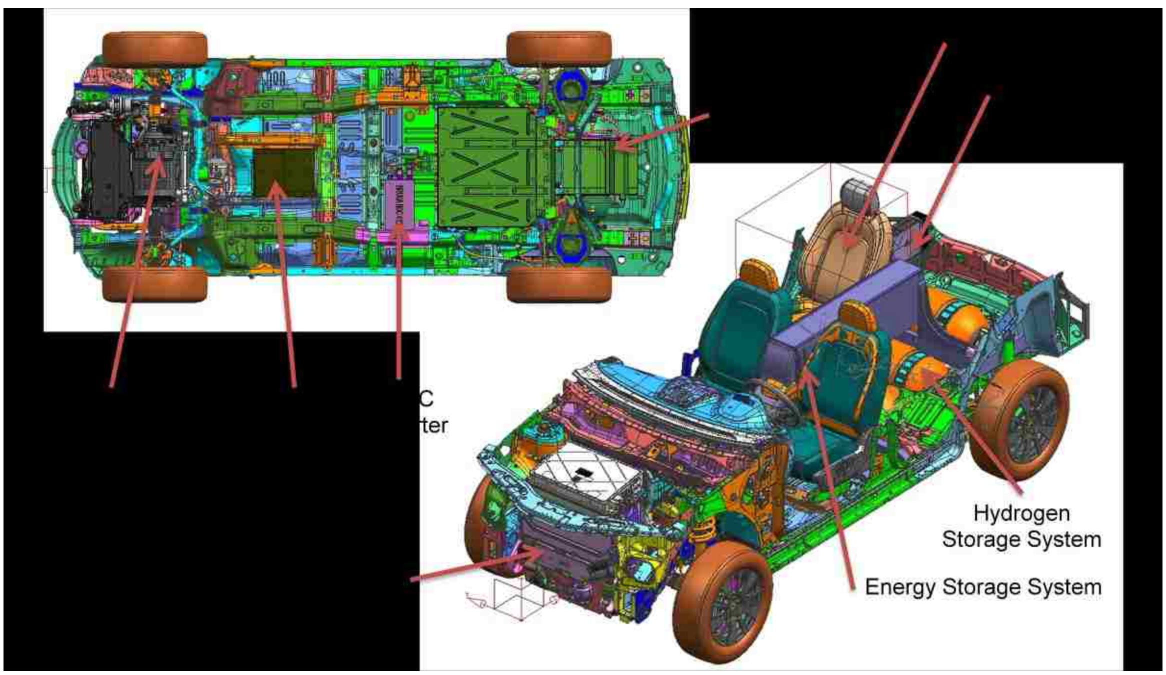

Figure 2.2. Fuel Cell Plug-in Hybrid Electric Vehicle

2.2.1. Vehicle Electrical Systems diagram of the vehicle architecture of the Missouri S&T EcoCAR has been included in Figure 2.3 [29]. This architecture requires two high voltage junction boxes: the GM Power Management Distribution Module (GM PDM) and the S&T designed Energy Storage Power Distribution Module (S&T PDM). The system contains four sets of contactors that allow the vehicle to operate in two different electrical modes; Electric Vehicle Mode (EVM) and Fuel Cell Hybrid Mode (FCHM). The EVM allows for the vehicle to operate with power from the ESS without using the dc/dc converter. This will improve the efficiency in this operational mode as no power used from the auxiliary loads (12V converter, A/C compressor, cabin heater, and front cooling fan) will be processed by the dc/dc converter. Finally these contactors will be controlled during grid charging of the ESS.

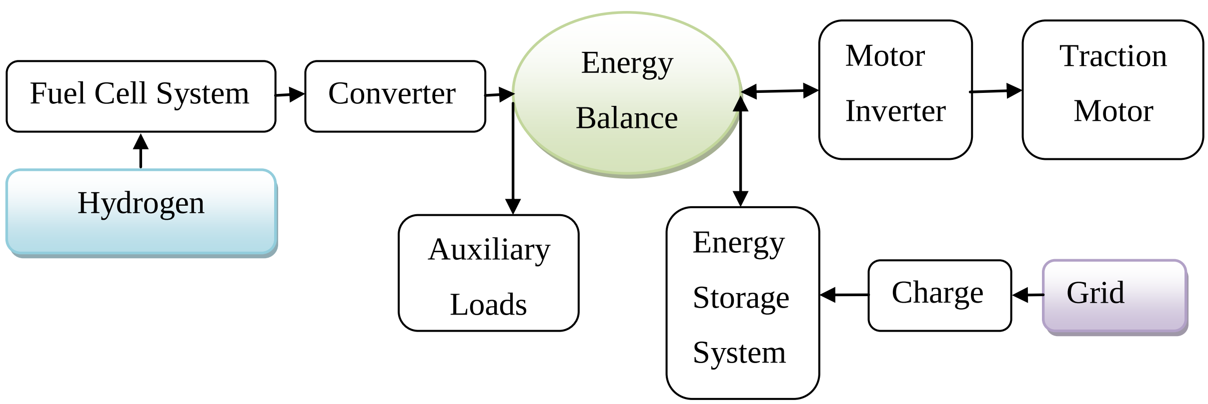

Figure 2.3. Missouri S&T High Voltage Architecture [29]

The A123 Systems Energy Storage System is connected to the S&T PDM. The S&T PDM allows direct connection of the ESS to the GM Electric Traction System for increased regenerative capability and improved performance of the ETS. The S&T PDM contains several contactors to allow the vehicle to run in a pure EV mode without the use of the bidirectional DC/DC converter and for a Fuel Cell mode in which the DC/DC converter is used to push power from the Fuel Cell system into the ESS or the ETS depending on road demand and control.

2.2.2. Vehicle Control Architecture This design includes three different control areas: the fuel cell power module (FCPM), the fuel cell propulsion system (FCPS), and the platform control system. The FCPM area contains all of the ancillary systems required to operate the fuel cell. The FCPS contains the system essential for power balance in the vehicle and the hydrogen delivery system. The platform area contains the vehicle safety system and human to machine interface system. The charge depleting cycle shows the low power use of the fuel cell with increase in the power demand to limit the discharge of the energy storage system. This discharge limit has been set at 1C (one hour discharge rate) or 16kW. In the charge sustaining operation, the fuel cell meets the average power demand of the vehicle for the drive cycle. The ESS DC/DC converter is limited to 28 kW sustained operation with peaking operation up to 40.5 kW based on thermal conditions. Therefore while in charge sustaining operation the fuel cell cannot act as a perfect power follower. The ESS will be required then to meet the balance of the power required. The vehicle operation has three propelling modes of operation: charge depleting, charge sustaining and all electric; with three braking modes: friction, all regenerative and hybrid which form the supervisory control strategy for the vehicle. The transitions are based on the ESS state of charge, acceleration power demand, deceleration demand, vehicle speed, time since fuel cell startup, and regenerative braking capability as determined by state of charge and current output power of the fuel cell. The decision of high velocity and high acceleration is generally based on the calculated power demand of the drive cycle and the duration of this demand [30].

2.2.3. Vehicle Hydrogen Storage System The Hydrogen Storage System (HSS) is in charge to store and provide hydrogen to the Fuel Cell system. The HSS is composed by three carbon composed cylinders with a layer of steel, high voltage heating system and safety devices. Each of the hydrogen cylinders has the dimension of ø391.5mm x 737.5 mm and a total mass of 191 kg. The hydrogen gas is filled in these cylinders by pressurizing at 700 bar and 15ºC. The HSS is able to store approximately 4 kg of hydrogen at the specified pressure.

The GM Equinox HSS cylinders are produced by Quantum Fuel Systems Technologies Worldwide [31]. Figure 2.4 [32] illustrates the different components of each of the hydrogen cylinders. In addition, GM research showed that the HSS is even more safe that gasoline tanks and at its location, is able to support forces up to 35 to 40 kN [33].

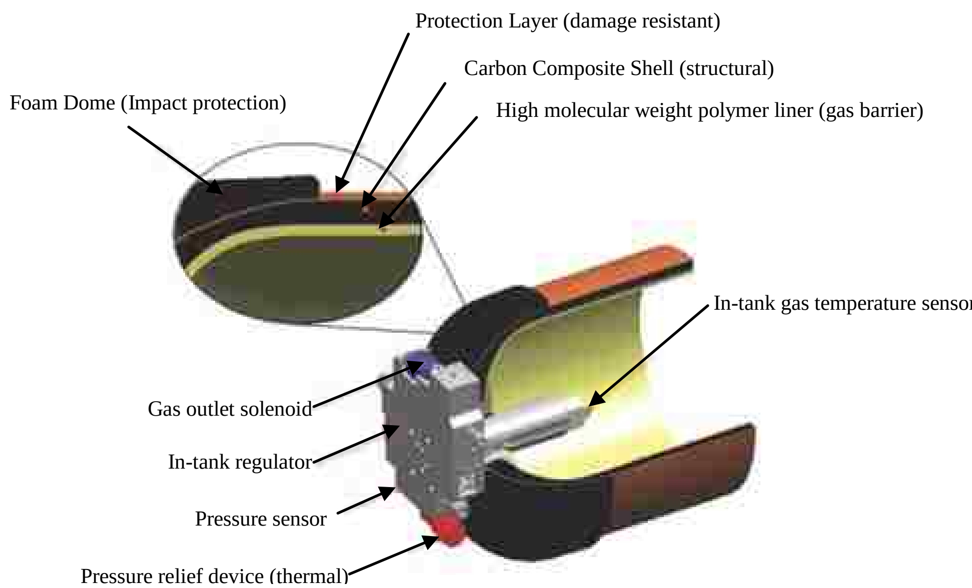

Figure 2.4. Hydrogen Storage System cylinders [32]

2.2.4. Fuel Cell Power Module Missouri S&T EcoCAR team is going to use a GM fuel cell system which includes the balance of the plant and the Electrical Traction System (ETS). The FC system has a peak power output of 95 kW and it has relatively low response time. The balance of the plant includes air compressors for the intake, air humidifiers, heaters and hydrogen inlet system. As it is well know the fuel cell system has a high rate of heat dissipation which implicates a complex cooling system that will be described in next chapter. The Fuel cell stack used for the team is presented in Figure 2.5 [34][35]. The total weight of the fuel cell system is 250 kg (without the cooling system) and has a volume of 405 liters; the stack has a volume of 104 liters and uses a total of 80 grams of platinum [36].

Figure 2.5. Fuel Cell Stack [34] [35]

2.2.5. Thermal Systems Missouri S&T EcoCAR has a complex cooling system which includes four loops. The cooling loops are: The high temperature cooling loop, the low temperature cooling loop, the electrical storage system cooling loop and the HAVC loop. Figure 2.6 illustrates the location of the cooling loops.

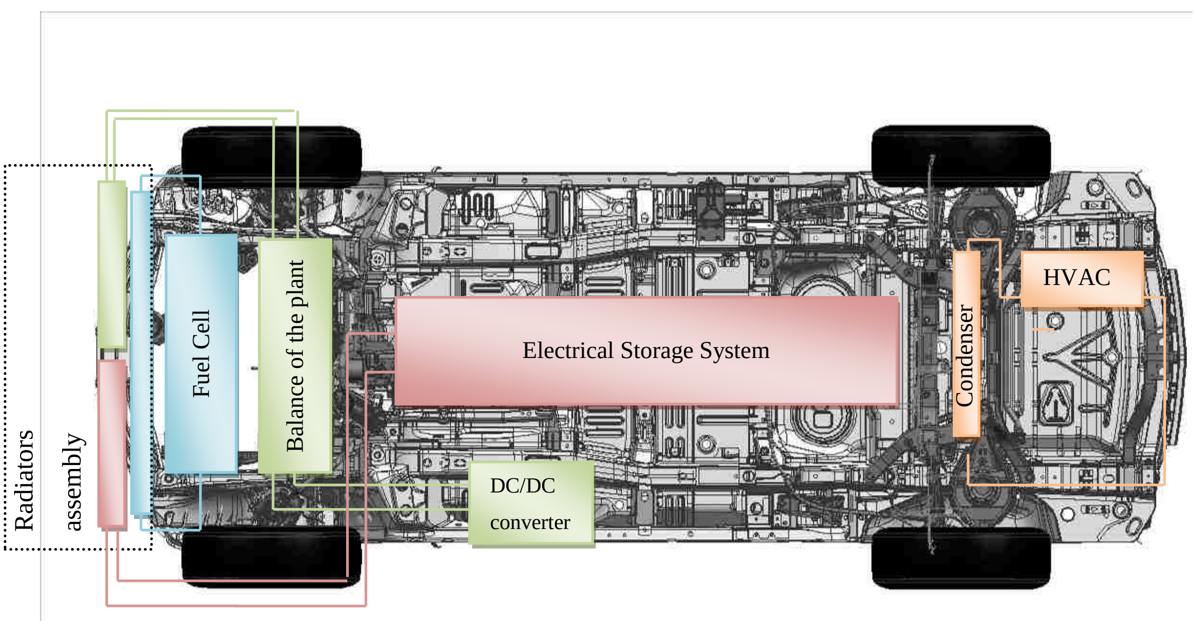

Figure 2.6. Missouri S&T FC-PHEV cooling loops

The first cooling loop is only for the Fuel Cell stack and is dominated as the high temperature cooling loop. The fuel cell stack has a very narrow operating range of temperatures; 80-85°C is the optimum temperature range, with 87°C as the maximum temperature. The components in the high temperature loop generate roughly 90 kW of heat at maximum operating conditions. Fuel cell rejects nearly all of the waste heat into the coolant, as opposed to internal combustion engines, which reject heat to the coolant and through the exhaust. This puts quite strain on the cooling system, so a very effective cooling system is needed.

Fuel cells are very sensitive to impurities; a special coolant has to be used to prevent contamination of the fuel cell. Currently, a low electrical conductivity coolant is used, with an ion exchanger in the coolant reservoir to maintain the low conductivity. Furthermore, in order to prevent impurities from harming the fuel cell, the radiator lines have to be vacuum brazed to prevent contamination from the flux used in brazing. Brass and copper fittings can also lead to impurities in the coolant, so they are not to be used.

The second cooling loop is the low temperature loop. This loop uses a mixture of 60% ethylene glycol and 40% water by weight. This fluid is commonly used in convective heat transfer applications. The systems that are on the low temperature loop include the high voltage bidirectional DC/DC converter, electric traction system, power management distribution system, and compressor unit. The components that are under our control as a team are the radiator, coolant pump, and coolant reservoir.

The third cooling loop is the electrical storage system loop. The team is using regular water glycol as the coolant and five cooling plates for each module. The radiator of this system will be located in the front of the vehicle and it will be couple with the radiators assembly.

Finally, the last loop is for the HVAC. Due the packaging of the ESS the HVAC blower has been removed and relocated in the trunk of the vehicle. The team is using a condenser in the modified rear cradle. Finally, the electrical AC compressor is relocated in order to provide more space for the fuel cell stack.

2.3. STRUCTURAL MODIFICATION

The team had to make several modifications to the vehicles structure in order to locate all the powertrain components. In order to install the Fuel Cell the team had to replace the current front cradle for a similar one in order to use the correct contact points of the fuel cell. The installation of the HSS was the component which required more modification than all.

The HSS is located in order to avoid any kinematics interference with the rear suspension and it had a body cutting area of 766 x 800 mm^2. The HSS was located as low as possible in order to allow an acceptable location for the Electrical Storage System (ESS) and keep the possibility to install the rear seats for consumer acceptability. There are seven components that are going to be either removed or modified and are going to be replaced with three beams showed in Figure 2.7.

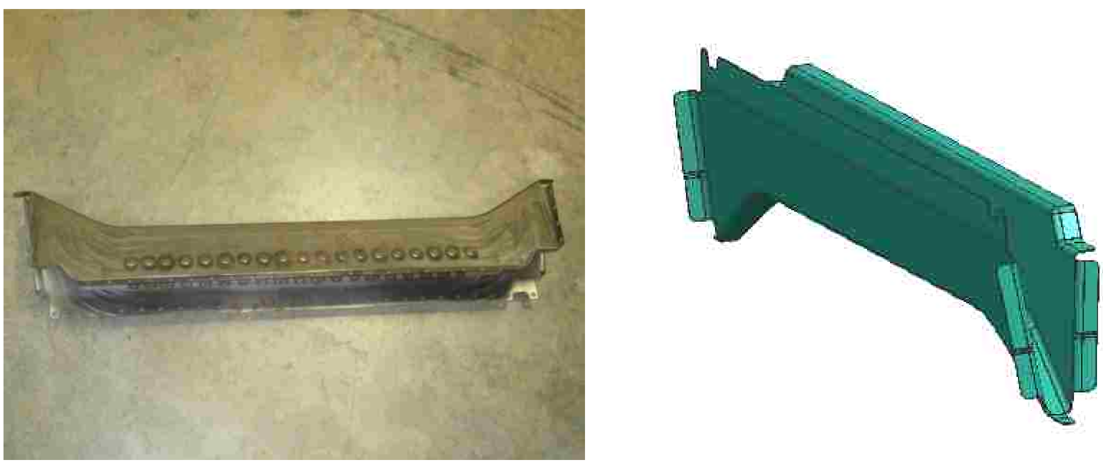

Figure 2.7. Crossing member reinforcements

3. ELECTRICAL STORAGE SYSTEM DESIGNTHIS

3.1. COMPONENTS AND SUBSYSTEMS

In order to have the Electrical Storage Battery operational, it needs several subcomponents in the high voltage electrical system. The main components of the ESS system are the high voltage charger, DC/DC converter, ESS Power Distribution Module, ESS Electrical Distribution System, ESS Battery Control Module, and the A123 prismatic modules. The ESS is composed by five A123 prismatic modules illustrated in Figure 3.1. [37].

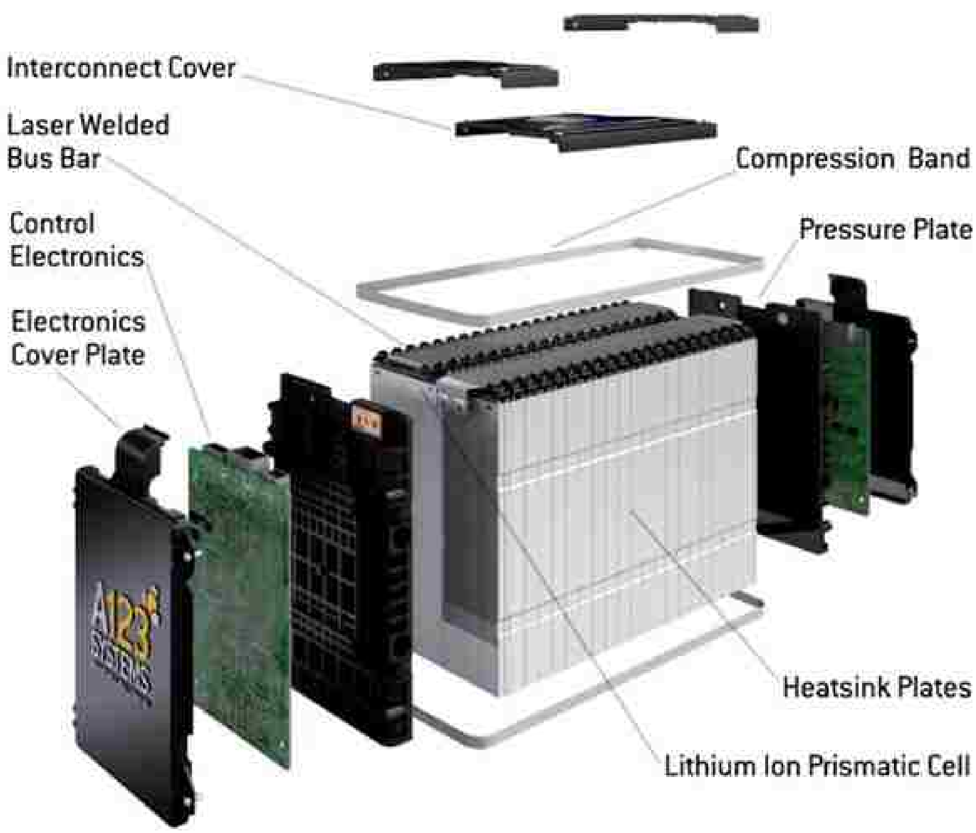

Figure 3.1. A123 prismatic modules components [37]

The ESS charger is located in the trunk of the vehicle; it is an air cooled system which will extract air from the posterior area of the rear wheel house. The high voltage battery charger NLG5 is manufactured by BRUSA® The low voltage battery will keep the same location of the Saturn VUE. Both components are presented in Figure 3.2. [38]. The ESS charger is the connection between the ESS and the grid.

Figure 3.2. High voltage charger [38]

In order to stabilize the high voltage electrical system, the FC-PHEV needs a DC/DC converter. Missouri S&T is using a BRUSA DC/DC converter 412, the component has the following dimensions: 433 x 156 x 100 mm^3 and has a mass of 10.25 kg.

The DC/DC converter is illustrated in Figure 3.3. It is important to note that this high voltage device has a pressure balance membrane to stabilize the inside pressure. The DC/DC converter will be located under the vehicle at the same level of the hydrogen cylinders bottom plate; it will be couple to the frame of the vehicle using a steel brackets. The location of the DC/DC converter will reduce the amount of high voltage wiring inside the vehicle.

The DC/DC converter is a liquid cooled devices, the inlets of the system is presented in Figure 3.3 [39]. The coolant requirements will vary according to the mode of operation. BRUSA® recommends different conditions and the team had access to experimental test of the converter. The team decided to couple this component to the low temperature cooling loop and run 4l/min and an inlet of 25°C-35°C.

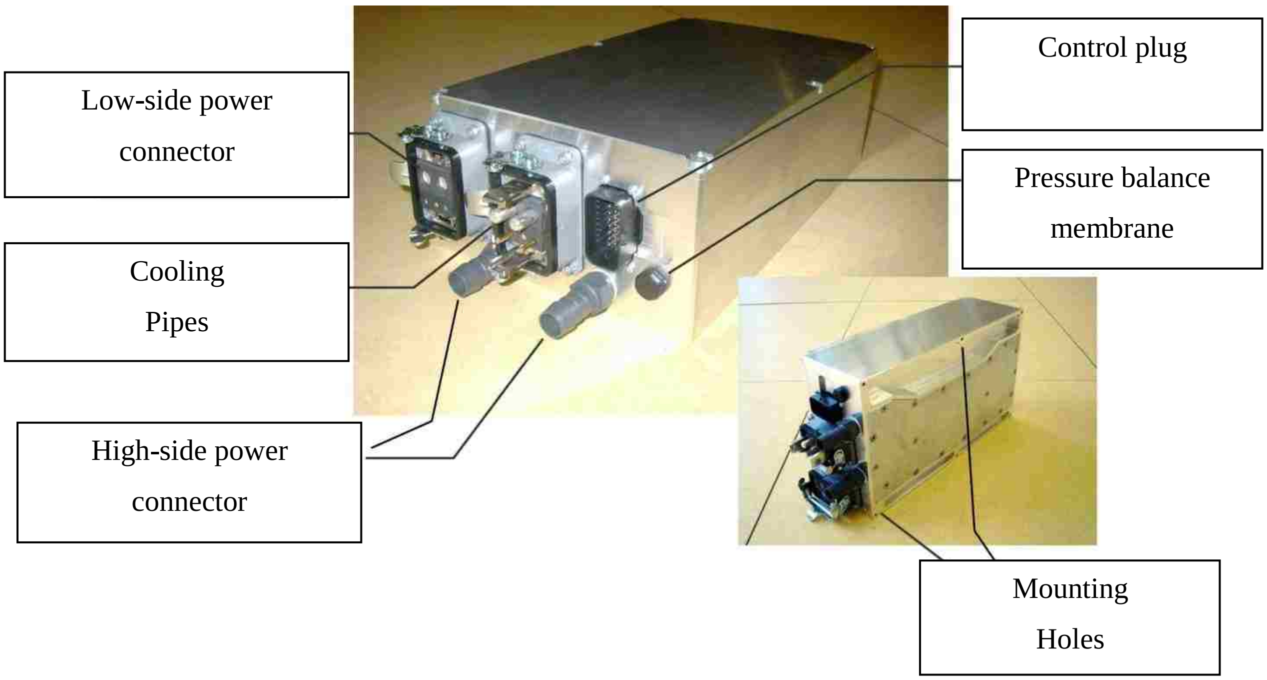

Figure 3.3. Image of Missouri S&T EcoCAR DC/DC converter [39]

Another important high voltage component is the Electrical Storage System Power Distribution Module (ESS PDM), the main function is to easily change between a Electrical Vehicle design to a Fuel Cell hybrid design. It is composed mainly of contactors, fuses and wiring. The location of this component will be next to the water vapor exhaust system under the vehicle.

Inside the pack there are two important components that allow the ESS pack to be electrical operational, the ESS Electrical Distribution Module that basically measures the current, measures the Hall Effect, and is composed mainly by contactors, resistors and sensors. The other important component in the pack is the Battery Control module that interacts with the main vehicle controller. Other components that the team needed to install in the pack are services disconnect switch and a high voltage fuse.

Finally, the ESS design for the vehicle contains the entirety of the system in the passenger cabin. Should an off-gas event occur it is essential that the design vents the hazardous gases out of the vehicle. In order to ensure that this occurs, the ESS enclosure has been designed with a rupture disk exposed to the environment with a gasket material used to seal the constructed pack. The specifications have been included below with datasheets in the appendix. The rupture disc is located in a plastic holder that is mounted in the bottom plate of the aluminum case. The Rupture Disk is designed for pressure relief valve applications, FIKE AD-80. The specifications are presented in the ANNEXE: A and it is illustrated in Figure 3.4. [40].

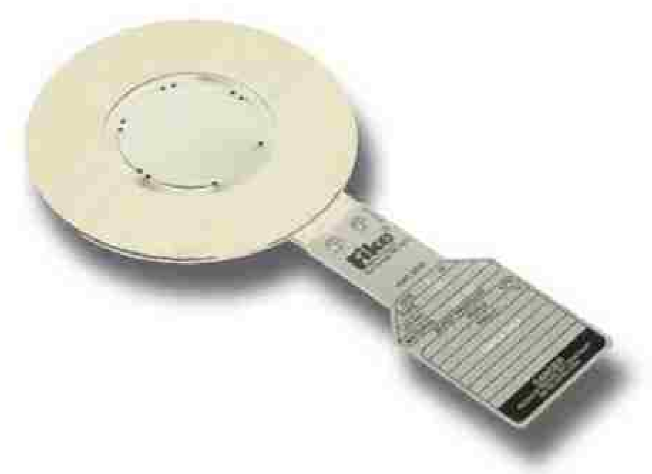

Figure 3.4. Rupture Disc [40]

The team will do a leak test to ensure the casing isolation, the procedure is described:

- Follow ESS assembly procedure alleviating the placement of all internal electronics and related devices
- Seal off cooling loop connections using screw caps
- Screw on pressure connection onto high voltage connection point
- Attach air compressor to pressure connection fitting

- Apply either Snoop or mixture of soap and water to all seals and joints
- Turn on air compressor and allow it to run until 5 psi is achieved with the ESS pack
- Turn off air compressor and check for bubble formation
- Monitor pressure gauge for 15 minutes to ensure no leakage has occurred

3.2. ELECTRICAL DESIGN

The electrical design developed by the team was mainly focused in the Electrical Storage System Power Distribution Module. A layout of this design is presented in Figure 3.5 [41]. The ESS PDM is focused to manage the power flows between the fuel cell bus, the battery, the traction motor, and any charging circuitry. In addition, the ESS PDM control the contactors that allow for both hybrid and battery only (EV) modes.

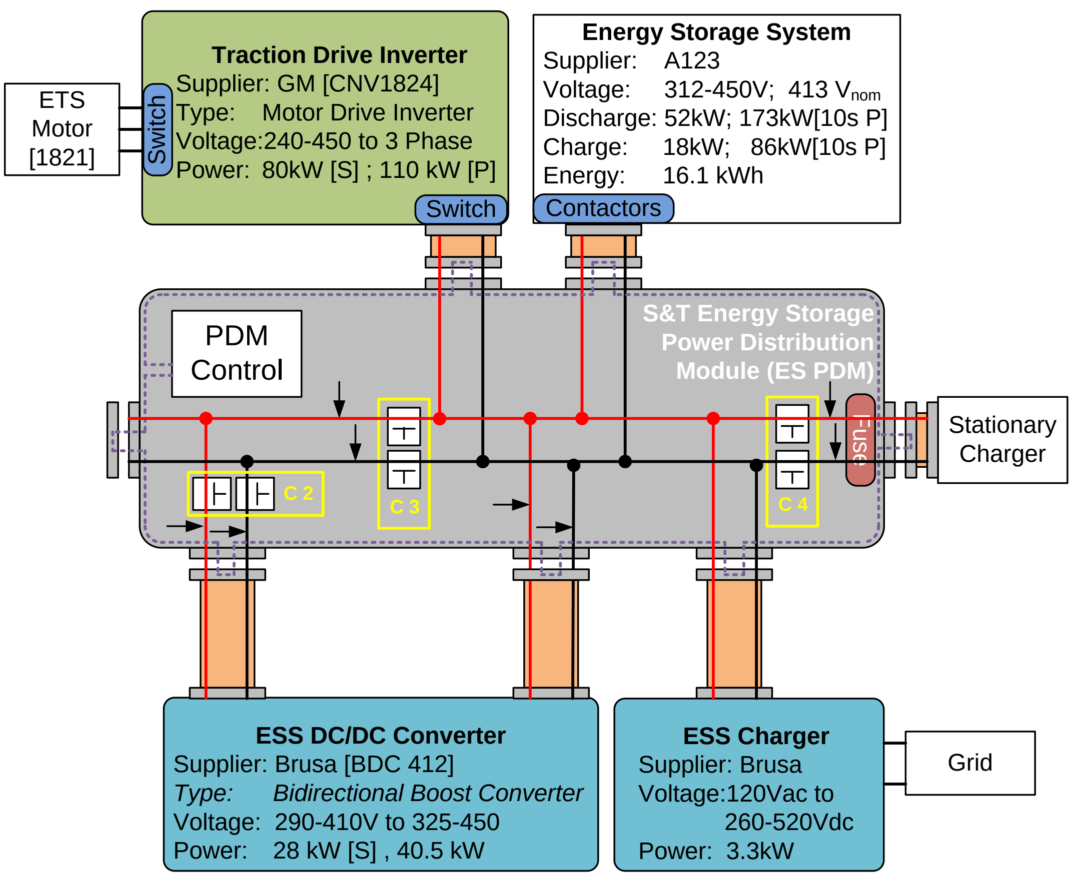

Figure 3.5. Energy Storage System Power Management and Distribution Module [41]

3.3. MECHANICAL DESIGN

3.3.1. CAD The main distribution of the pack is shown in Figure 3.6, as it can be seen five modules will be located in two rows, with two upper modules and three lower modules. The case will be designed to be airtight with enclosures covering a strong understructure (gray). The case has three removable parts as it can be seen in bottom part of Figure 3.6. The central removable part has metal rails that allow for easy maintenance removal. This removable cover is made of thin steel and will be lined with a rubber gasket to ensure the airtight seal. In addition, two more removable compartments are presented; each one will be removable in the direction showed.

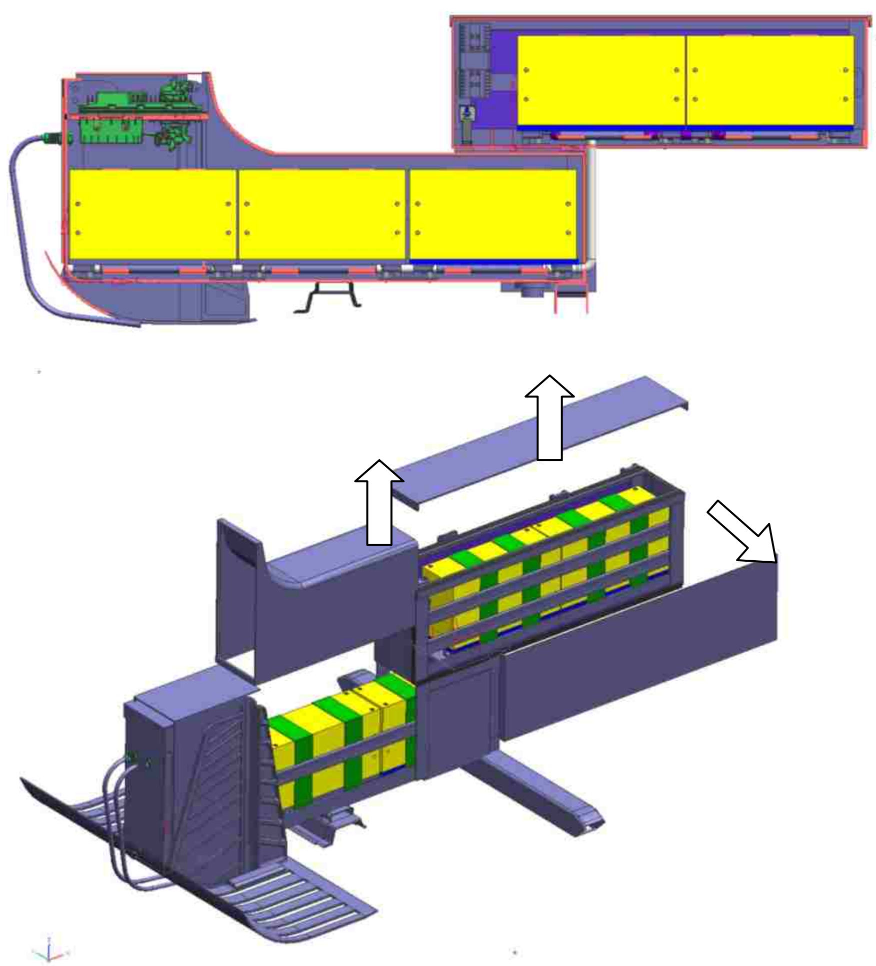

Figure 3.6. ESS Distribution

The main cover will be secure by bolts to the structural frame and will feature a special inlet shape for driver comfort; Figure 3.7. Casing details of the ESS presents details of the design. In order to ensure airtight there will be several bolts installed.

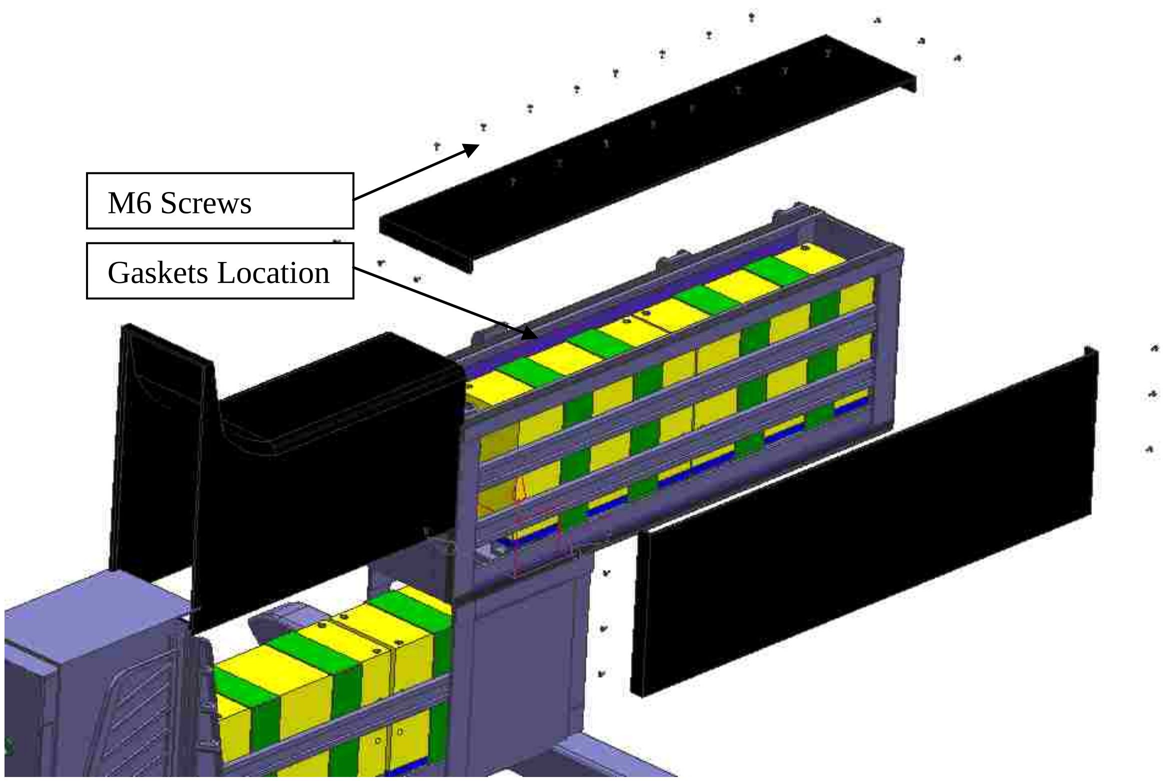

Figure 3.7. Casing details of the ESS

The other faces of the case will be welded to the structure to assure stability. The ESS has two main sub-systems, the electrical packaging and the cooling system packaging:

Electrical Packaging, The main components of the electrical system are the BCM and EDS, shown in green in Figure 3.8, they are located next to the external pack connector. Moreover the manual service disconnection and the high voltage fuse will be located with the upper modules. The manual service disconnection and the fuse are electrical isolated to the case. The location of the manual service disconnection is accessible through the top removable case of the second section of the pack. Between the modules there will be a special HV connection in order to reduce the unnecessary wire. The manual service disconnection will be pulled to the top of the battery pack. The BCM and EDS are located in a removable plate. Finally this system is completely isolated from the others, i.e. if there is leaks in the cooling system there will not a form to touch the electrical system.

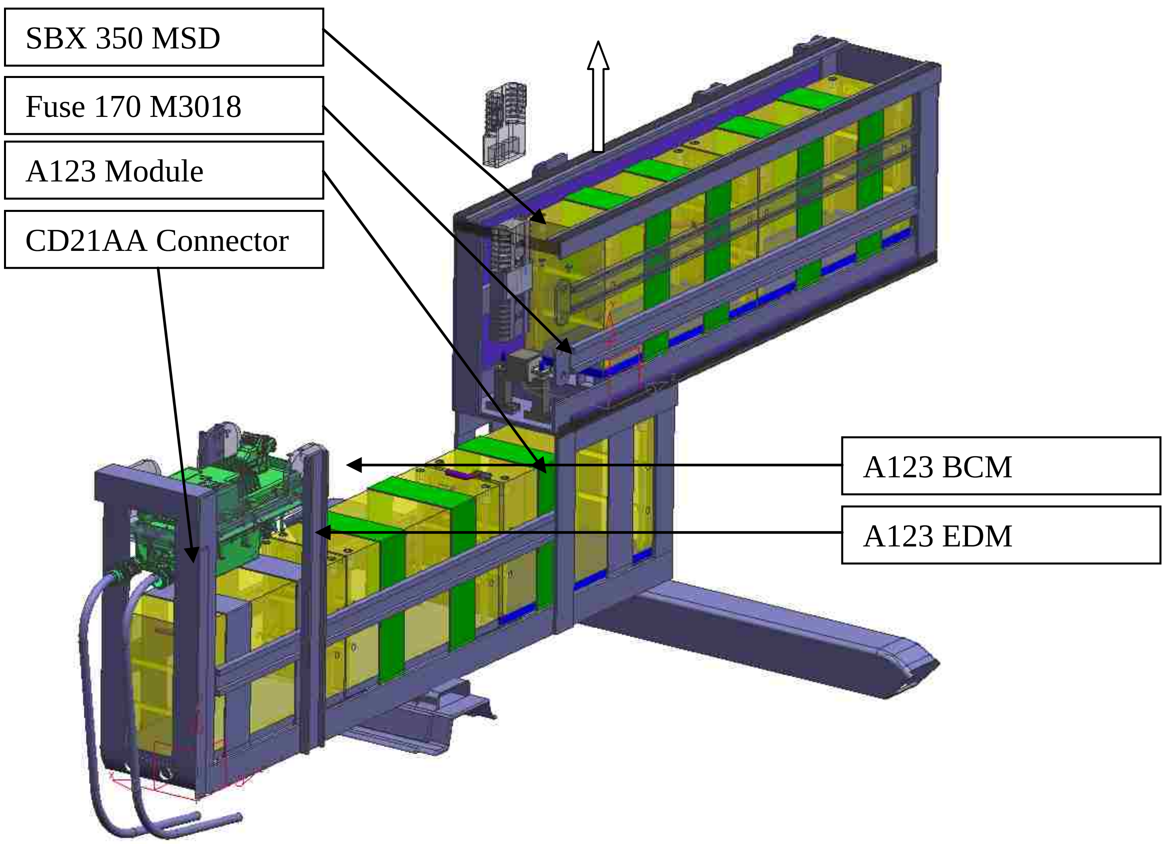

Figure 3.8. Electrical System Packaging

Cooling System, The cooling system has two sets of cooling plates, each of one connected in parallel Figure 3.9 shows the inlet and outlet of the cooling plate system. The first set of cooling plates has three plates interconnect with a 1 in. hose. The second set of plates will have similar configuration but with only two modules. Each manifold has eight entrances to the cooling plate with 5 x 5 mm^2. The aluminum plates will be supported on top of the structural plate. The space that this structural plate provides will hold the hoses and the manifolds of the cooling plates. The connections of the cooling plates set will be outside the casing in order to avoid contact between the HV system and the cooling system.

Finally in order to reduce the thermal resistance between the plate and the module thermal grease will be located on top of the cooling plate.

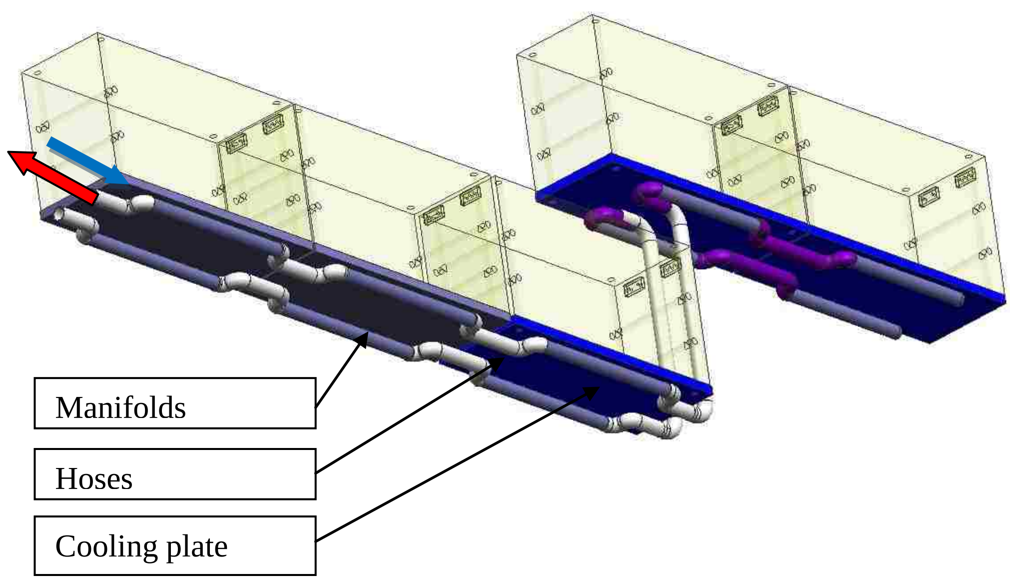

Figure 3.9. Cooling plate assembly

3.3.2. Mounting Concept Each pack of module will be hold on top of a battery structural plate, which will hold the selected vibration isolators. The vibration isolators are going to go through the pack. These vibration isolators will be connected to the Structural Plate B which will work as a mechanical connection with the modules bolts.

Finally the 4 hardened bolts (class 12.9) and the locking nuts will be located under the cooling plate in the Structural Plate B. The first structural plate will have hooks in the sides in order the hold two straps per modules. The configuration of the top plate is illustrated in Figure 3.10**.** In addition four nylon straps will hold each module; this should hold up to 60 kg of force. The straps will be tied to the reinforcement structure. The nylon webbing straps are 3 in with a thickness of 0.5 in.

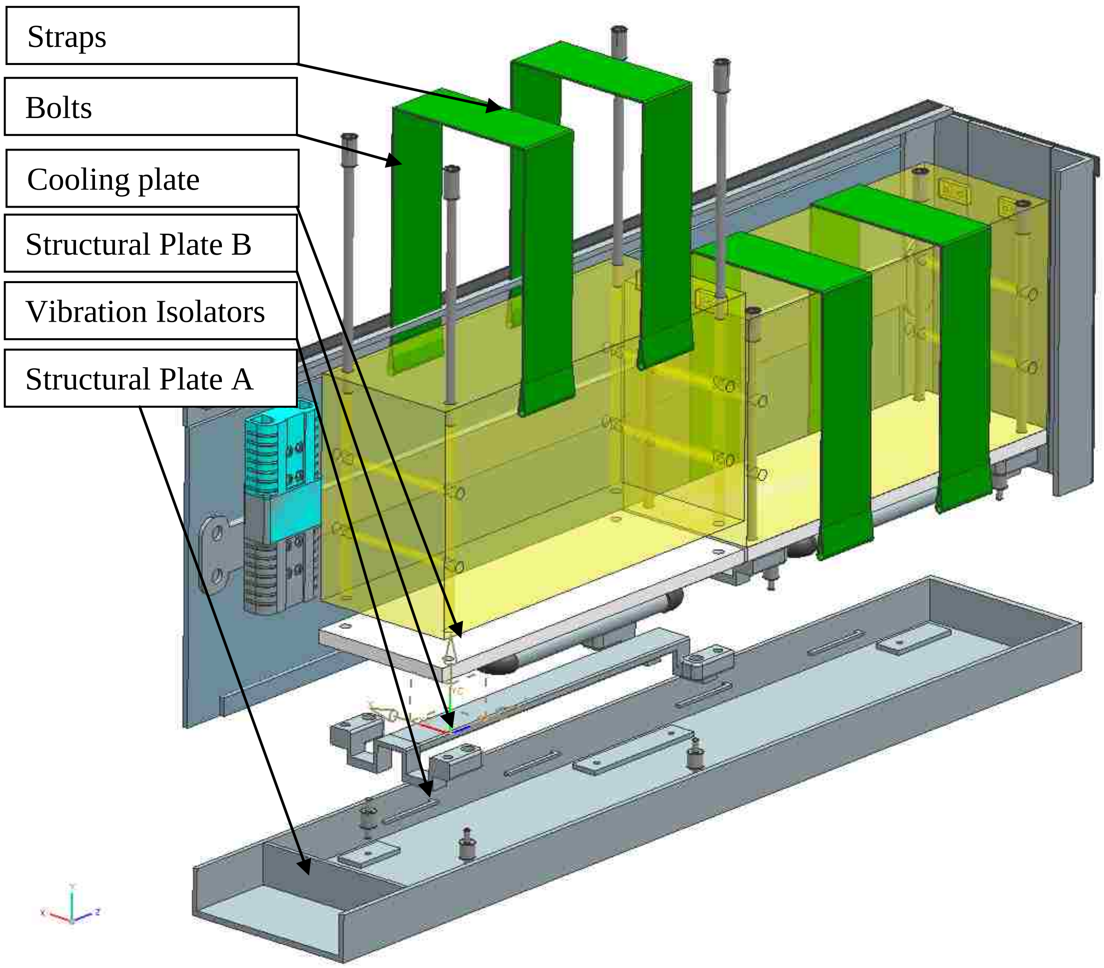

Figure 3.10. Mounting concept for each Module

3.3.3. Structural Analysis The structural analysis has been done by considering an acceleration of 20 g in the X-direction, 8 g in the Y direction and 20g in the Z-direction. The center of gravity was initially calculated and it is located at the point (1126, 225, 0) mm. For the acceleration in X-direction, the force is estimated to be 39,240 N. The reaction forces generated by this force have been calculated at each support point i.e. A, B, C and D and E. Figure 3.11 illustrates the brackets locations.

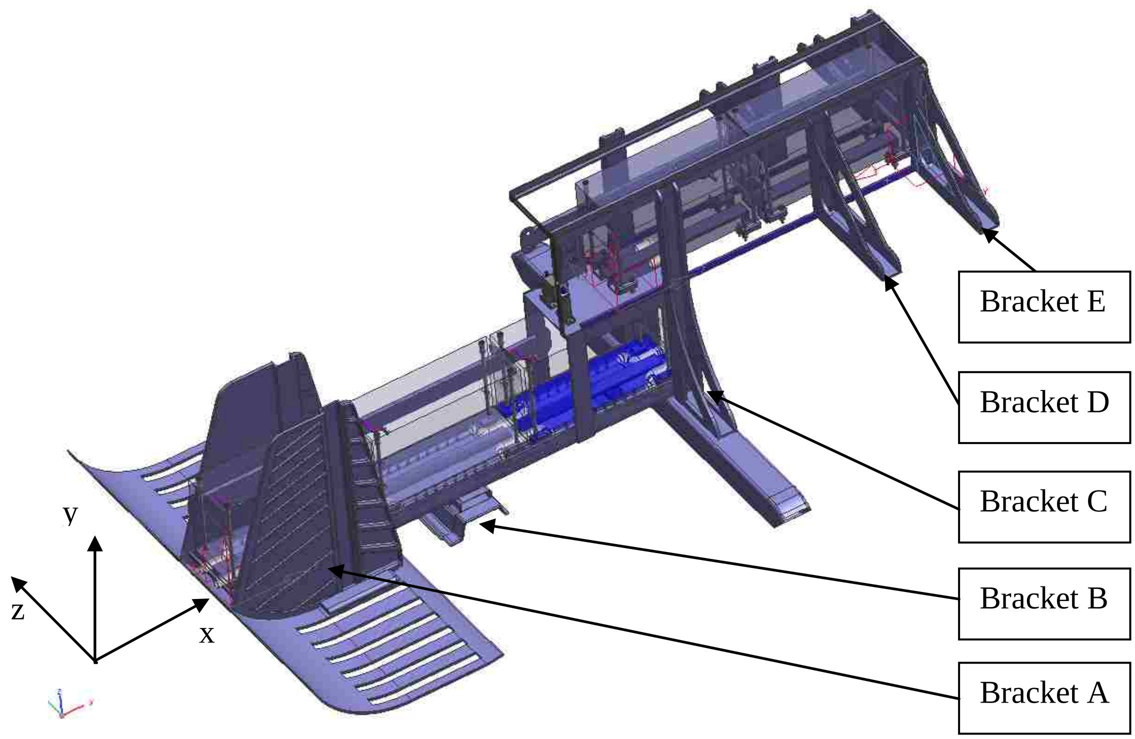

Figure 3.11. Brackets in the electrical storage system

The analysis was divided in two steps, the first step was to determinate the forces actuating in each contacts point of the case as a single box, then with the actuating forces design the dimensions of the brackets. Finally the crossing members were analyzed to ensure the location of the ESS modules. In the present documents the forces, momentous, finite element analysis and factor of safety are illustrated.

The forces and moments caused due to the acceleration of 20 g in the X-direction at points A, C, D and E are tabulated in Table 3.1.

Table 3.1. Pressure and moments at points A, C, D and E in X direction

POINTS:	**A**	**C**	**D**	**E**
PRESSURE (N/m^2)	98888.8	-2591.92	7.822*10^5	2.723*10^3
MOMENT (Nm)	4175.57	- 53.878	- 13451.85	-62.604

The forces and moments caused due to the acceleration of 8 g in the Y direction at points A, C, D and E are tabulated in Table 3.2.

Table 3.2. Pressure and Moments at A, C, D and E in Y direction

POINTS	**A**	**C**	**D**	**E**
PRESSURE (N/m^2)	49922.66	-48717.94	0.340*10^6	-2723.04
MOMENT (Nm)	-2107.98	1012.7	5859.25	62.6

The forces and moments caused due to the acceleration of 20 g in the Z-direction at points A, C, D and E are tabulated in Table 3.3.

Table 3.3. Pressure and Moments at A,C, D and E in Z direction

POINTS:	**A**	**C**	**D**	**E**
PRESSURE (N/m^2)	-72.018*10^6	66.84*10^6	141.99*10^5	-8.65*10^6
MOMENT (Nm)	3.04*10^6	1.389*10^6	-2.44*10^5	-1.99*10^5

The forces and moments caused due to the acceleration of 20 g in the Negative X-direction at points C, D and E are tabulated in Table 3.4.

Table 3.4. Pressure and Moments at C, D and E in negative X direction

POINTS:	C	D	E
PRESSURE (N/m^2)	- 350.085 * 10^3	-267.71*10^3	-133.855 * 10^3
MOMENT (Nm)	-7277.22	4603.90	3.077*10^3

The forces and moments caused due to the acceleration of 8 g in the Y-direction at Support B are calculated to have a pressure in the top surface of 145.982 x 10^3 N/m^^{2} and a momentum due the distance to the center of gravity of 1.471 x 10^3 N.m

Moreover, the forces and moments resulting on the hook due to the acceleration of 8 g in the Y-direction are 1.502 x 10^6 N/m^2 considering four hooks per module. The straps were selected to support the tensile forces.

The removable side supports as shown in will support the 20 g acceleration situation for two modules. The bracket will hold up to two battery packs (35 kg each) times 20 g which is a force of 1,374 N.

Using the forces and moments calculated a Finite Element Analysis was performed using ANSYS®. The element used for the structural analysis is an 8-node 185 Solid element. The material considered is Structural steel - ASTM-A36 whose Young's modulus is 200 GPa and the Poisson's ratio = 0.3.

Figure 3.12 illustrates the finite element analysis of Bracket A.

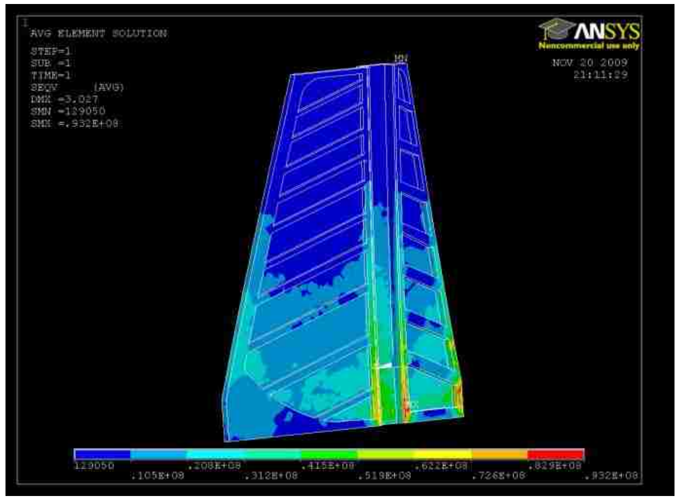

Figure 3.12. Finite Element Analysis results of Support A

The maximum values of the deformation and stress for support A are 0.674 mm and 0.15 x 10^9 N/m^2 respectively. The Factor of safety (FOS) is given by the ratio of Ultimate strength to the applied stress. Ultimate strength of steel is 550 MPa. Thus FOS = 3.66. Thus the design is optimal and the FOS is within the specified range.
The FEA of Bracket C using the loads and constraints are illustrated in Figure 3.13.

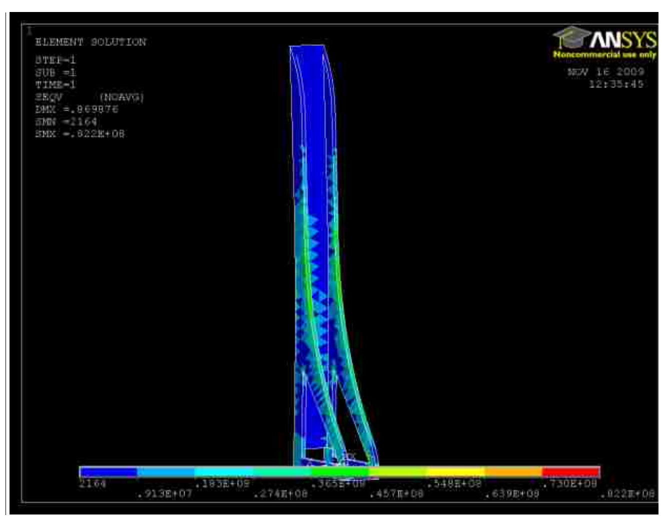

Figure 3.13. Finite Element Analysis results of Support C

The maximum values of the deformation, stress and strain for Support C are 2.162 mm and 0.822 x 10^8 The Factor of safety (FOS) is given by the ratio of ultimate strength to the applied stress. Ultimate strength of steel is 550 MPa. Thus FOS = (550 x 10^6)/(0.822x10^8) = 6.690. Thus the design is optimal.

The FEA of Bracket D using the loads and constraints are illustrated in Figure 3.14.

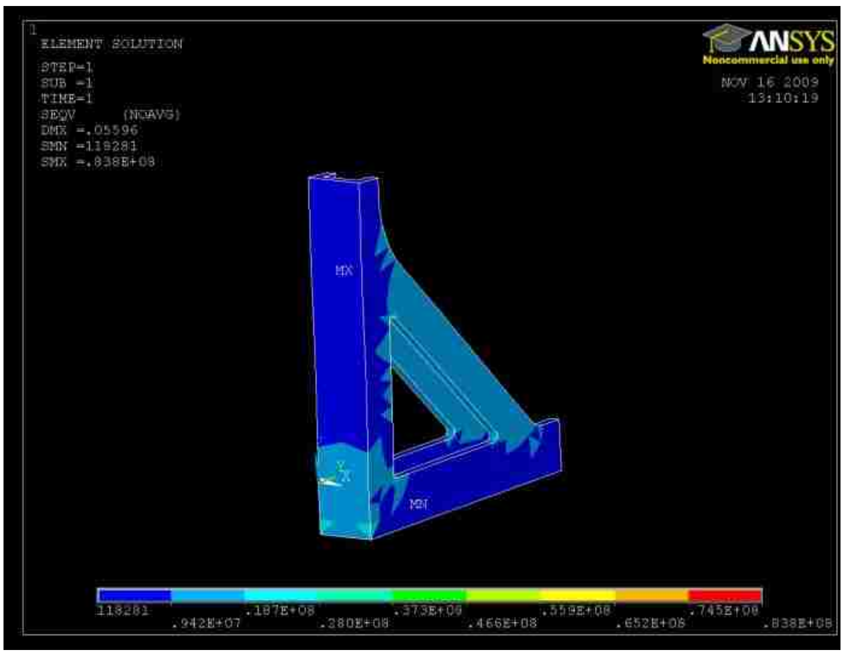

Figure 3.14. Finite Element Analysis results of Support D

The maximum values of the deformation, stress and strain for Support D are 2.929 mm and 0.838 x 10^8. The FOS is 6.563. Thus the FOS is within the specified range and the design is optimal.

The FEA of Bracket D using the loads and constraints are illustrated in Figure 3.15.

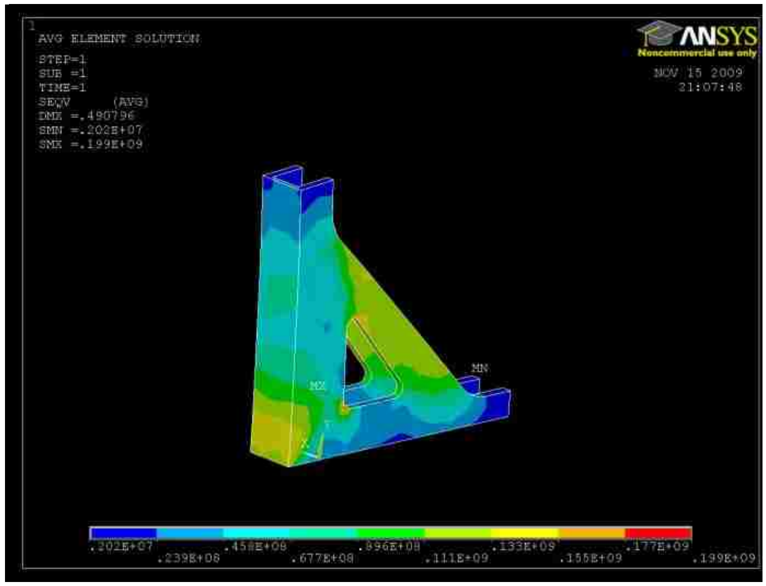

Figure 3.15. Finite Element Analysis results of Support E

The maximum values of the deformation, stress and strain for Support E are 0.110 mm and $0.199x10^9$ N/m^2, the factor of safety is 2.763. Thus the design is optimized. Similarly the FEA of Bracket C is performed and it is illustrated in Figure 3.16.

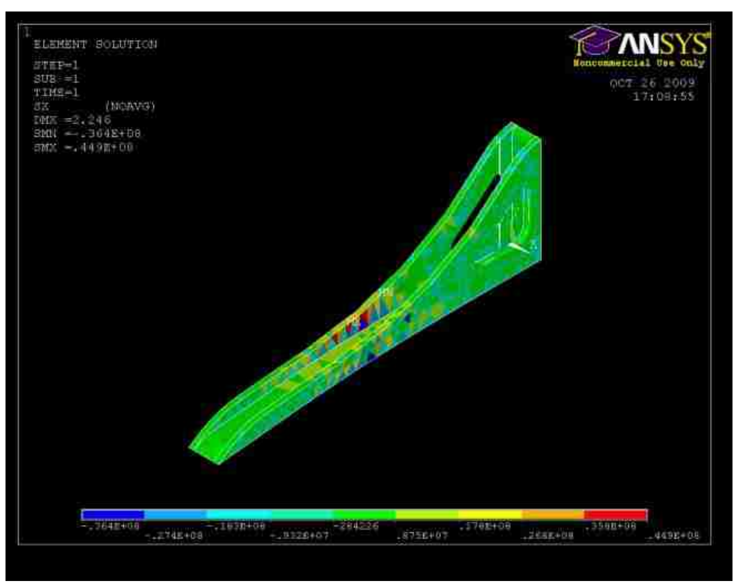

Figure 3.16. Finite Element Analysis results of Support C

The maximum values of the deformation and stress for Support C are 7.06 mm and 0.449 $x10^8$ N/m^2. The Factor of safety (FOS) is 12.25. Thus the design of the Support C is optimal.The analysis of Bracket B is presented in shown in Figure 3.17.

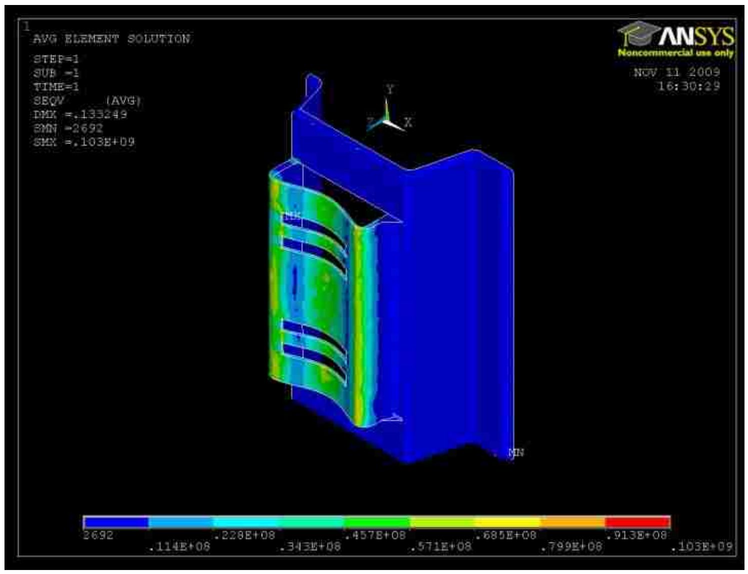

Figure 3.17. Finite Element Analysis results of Support B

The maximum values of the deformation and stress for Support B are 1.561 mm and a maximum stress of $0.103x10^9$ N/m^2. The FOS is 5.34, thus the design is optimal and the FOS is within the required limits.

In addition all main internal components were analyzed. The hooks located in the structural plate supporting the nylon straps holding the battery modules are presented in Figure 3.18.

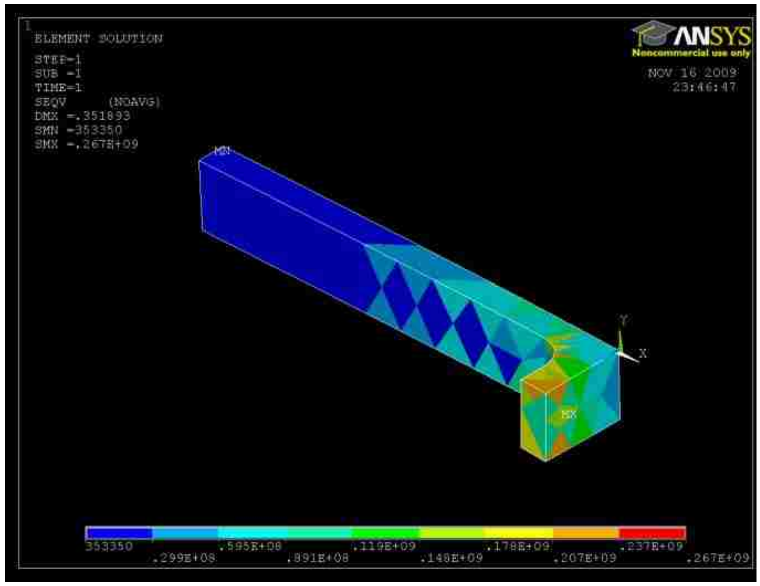

Figure 3.18. Finite Element Analysis results of the Hook

The maximum values of the deformation and stress for the hook are 1.766 mm and 0.267x10^9 N/m^2. The factor of safety is 2.06.

Finally, Figure 3.19 illustrates the analysis of the crossing members in the case. The FOS of this element is 32.7 however this is not a relevant parameter. The displacement on the other hand has to be reduced; this member has a displacement of 7.5 mm adding two of those support will ensure the displacement.

Figure 3.19. Removable side support

Table 3.5 is the summary of the FEA performed on the supporting brackets, hook and the removable side cross member in X, Y and Z directions respectively.

Table 3.5. FEA Summary

Actuating force direction	ITEM	Maximum Stress (N/m^2)	Maximum Deformation (mm)	Factor of Safety
X-direction	Support A	0.150×10^9	1.301	3.666
	Support C	NA	NA	NA
	Support D	0.838×10^8	2.929	6.563
	Support E	NA	NA	NA
Y-Direction	Support A	0.755×10^8	0.674	7.284
	Support B	0.103×10^9	1.561	5.34
	Support C	0.822×10^8	2.162	6.690
	Support D	0.502×10^8	4.98	10.95
	Support E	NA	NA	NA
	Hook	0.267×10^9	1.766	2.06
Z-Direction	Support A	NA	NA	NA
	Support C	0.223×10^8	18.63	24.66
	Support D	0.250×10^9	12.986	2.2
	Support E	0.199×10^9	0.11	2.76
	Removable side cross member	0.162×10^8	7.5	32.7

3.3.4. Vibration Analysis

The recommendation of the battery manufacture is to have a system of natural frequency more than 50 Hz in combine with the vibration isolators. The team decided to uses four vibration isolators per module. The weight of each module is almost 16 kg.

After a selection process the team selected a cylindrical vibration isolator which has a spring rate than 8.8 kg /mm. The static deflection is 0.6 mm and a natural frequency of 20.4 Hz. The selected vibration isolator is illustrated in Figure 3.20. The diameter (A) is 5/8", height (B) 5/8", the thread length (C) (D) is ½". The compression spring rate is 370 lbs/in.

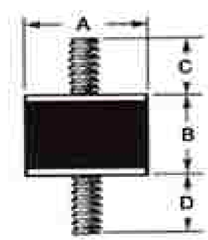

Figure 3.20. Vibration isolator

3.4. THERMAL ANALYSIS

The FC-PHEV has four cooling loops in the design: low temperature cooling loop, high temperature cooling loop, electric storage system cooling loop and AC system.

The primary functions of these cooling loops are to maintain the heat producing components within the optimum operating conditions. The high temperature loop takes care of the fuel cell stack, while low temperature cooling loop take care of the thermal loads of DC/DC converter, ETS, and PDM. As the ESS cooling loop is taking care of the battery pack cooling, the rest of this report concentrates on this loop. The architecture of these cooling loops is as shown in Figure 3.21. The radiators' locations are presented in green.

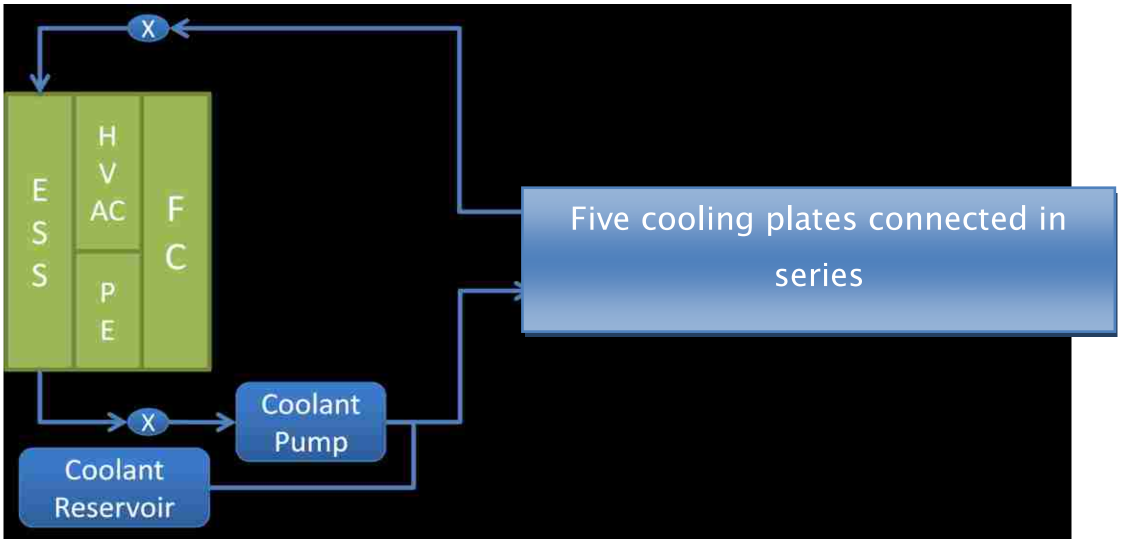

Figure 3.21. The ESS cooling loop

The high temperature flow which carries the heat produced from the battery modules is fed directly to the radiator pack through a reducing valve. The function of the reducing valve is to increase the heat transfer rate in the radiator. The radiator pack consists of four different radiators and a fan to provide the necessary air flow rates into the radiator. The stack consists of the ESS radiator, HVAC, Power electronics, and Fuel cell radiator. All the radiators use water glycol mixture except the fuel cell radiator. Fuel cell radiator is a custom build radiator which uses de ionized water as the coolant. All other radiators are already installed in the Saturn VUE provided by GM to Missouri S&T.

In order to determine the heat loads of each battery module, a simulation based on the drive cycle is done over a period of time. The drive cycle chosen is based on the worst case scenario of producing maximum heat. The team ran the drive cycles in the Simulink® model and determines the load requirements for the drive cycle at different operating conditions. For example, the top graph in Figure 3.22 represents the power requirement of the battery pack over the US06 drive cycle. The Powertrain System Analysis Toolkit PSAT models were used to complement the conditions of the analysis.

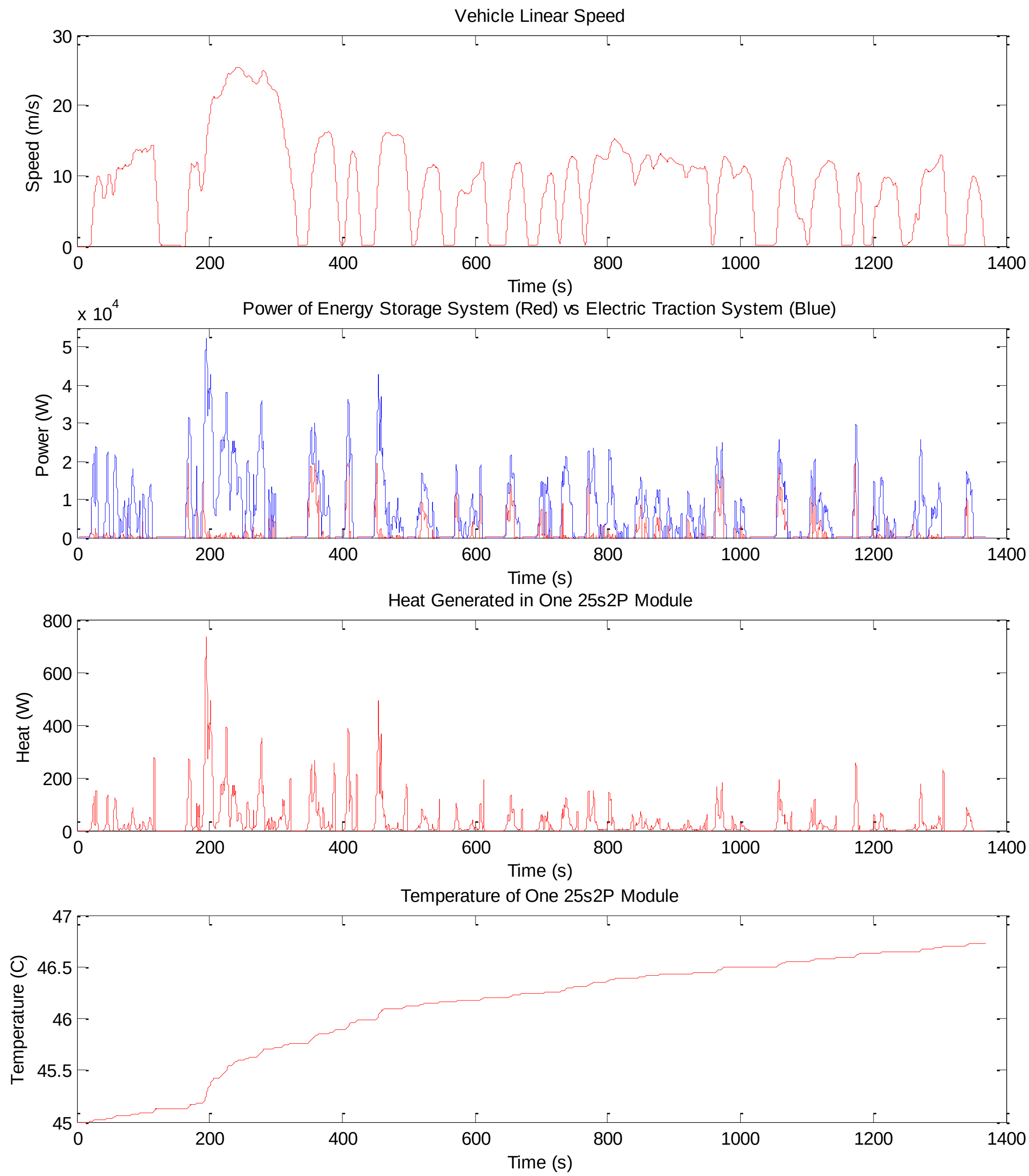

Figure 3.22. US06 Drivecycle PSAT and Simulink Simulation

It can be inferred from the simulation that the RMS value of the power requirement from the entire battery pack is 33 kW or a 2C discharge. Then the power flow from the entire battery pack for the drive cycle is also determined as shown in second graph.

From the resistance values provided by A123 Systems, we determine the heat generated in each module and for the entire pack using the equation:

$$Q = I_{rms}^2 \ R_{dc} \quad (1)$$

Where, Q is the heat generated in watts, I is the current flow in amperes and R is the resistance in ohms. Moreover, Figure 3.22 shows the heat loads produced from each modules and the entire pack respectively for the drive cycle. The RMS value of the heat produced is then determined and is found to for the entire pack and for each module. The cooling design for the battery modules is based on these values. The maximum thermal load produced in the module is for a very short period of time, about 10 seconds. Therefore we take care of these maximums by increasing the flow rates in the control strategies.

The temperature profile of the battery pack is then calculated from the heat produced at different ambient temperatures. Figure 3.22 shows the temperature profile for the battery pack of different ambient temperature of 45^{o}C, which is considered to be worst case scenario of driving in a desert. The changes in resistance in the battery pack with respect to change in ambient temperatures are not taken into account due to the lack of information.

Table 3.6 compares different drive cycles US06, LA92, UDDS, and HWFET for different operating conditions of Charge Depleting (CD), Charge Sustaining (CS), and Electric Vehicle (EV) modes at 45 ^{o}C. By examining the heat loads produced in the drive cycles it can be inferred that heat is generated at very high rate when the vehicle is running in EV mode. Also US06 produce the maximum amount of heat. This is considered as the worst case scenario, i.e. US06 operating in EV mode at 45 ^{o}C ambient conditions.

Table 3.6. Heat and Power Demand for Different Drive cycles and Mode of Operation

Drive Cycle	**CS@ 45^oC in Watts**			**CD@ 45^oC in Watts**			**EV @ 45^oC in Watts**		
	RMS Heat	Max Heat	RMS Power	RMS Heat	Max Heat	RMS Power	RMS Heat	Max Heat	RMS Power
US06	456	4308	11684	298	1387	12985	2549	22223	32057
LA92	301	4384	8136	181	693	8724	833	6865	17316
UDDS	132	1357	5393	103	528	5848	374	3667	10915
HWFET	211	2520	5916	159	489	9022	515	2609	16398

CS = Charge Sustaining mode, CD = Charge Depleting mode, EV = Electric Vehicle mode

It can be seen that US06 drive cycle is producing the maximum amount of thermal energy during the operation. We consider the worst case scenario of driving the vehicle in a desert with all the power demand is met by the batteries. That is the vehicle is running in electric vehicle mode. It can be seen that for this scenario, the total thermal loads produced is 2549.8 W. Thus, each of the modules are producing approximately 510 W of thermal energy. The internal thermal resistance value of the battery cell is 4.8 ^oC /W. This value is a very high number which provides insulation for the heat to be transferred into the cold plate. Therefore the cold plate should be kept at a very low temperature in order to provide the necessary potential of heat flow into the cold plate and reject heat. The heat transferred into the cold plate thus depends on the temperature on the cold plate.

Reviewing the state of art of cooling plates, it was determinate that the best way to cool the batteries is to run several small serpentines thought an aluminum cooling plate. The bottom part of the module is used as a contact point for the cooling plate. In addition, module has aluminum plates between the cells that allow a better flow of heat. It is important to note that the module has a high thermal mass that make difficult to cool the battery system in an EV mode at 45^oC.

For the cold plate design of the ESS, Missouri S&T EcoCAR team uses channel flow in serpentines inside the cold plate as shown in Figure 3.23. Each module has eight serpentines that are connect to a manifold. The plates are connected in series but the serpentines are connected in parallel.

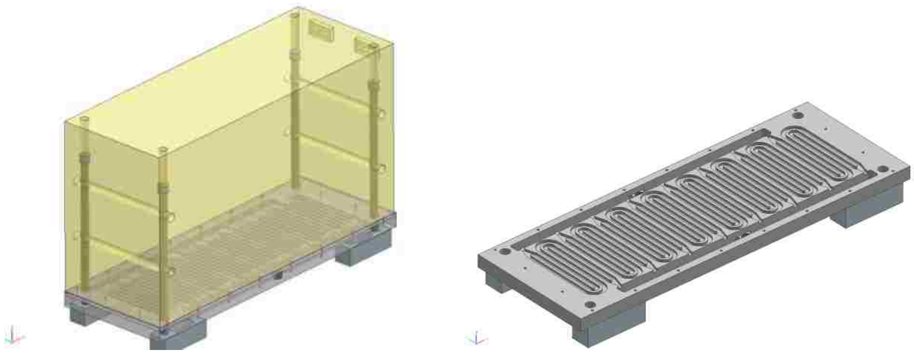

Figure 3.23. Cooling plate design for each module

3.5. FAILURE ANALYSIS

In order to perform a correct failure analysis of the Electrical Storage System, Missouri S&T EcoCAR team is developing a Fault Tree Analysis to identify all the possible events and the consequences in the ESS operation. Missouri S&T used BLOCKSIMS 7® part of the family ReliaSoft Office as the software tool. Blocksims allows the user to perform a deductive and inductive analysis. There are several blocks that the software provide the users such as the "OR", "AND", "INHIBIT", "TRIGGER EVENT". The top event is identified as the failure of the Electrical Storage System. Since the ESS is an integration of several systems, some of them mechanical, electrical, and controls the ESS failure has to be related with any of those systems. Figure 3.24 presents the three first levels of failure of the Electrical Storage System. The ESS failure is defined as failure in operation or safety. The assumptions of the ESS FTA are:

- The FTA is considering a steady state of operation

- All the components will be assumed to be in the useful life in the bathlub curve, the error of this assumption will cause a possible failure in the production part of the curve.
- The FTA is using a hardware approach.
- The ESS is already located in the vehicle and operational.

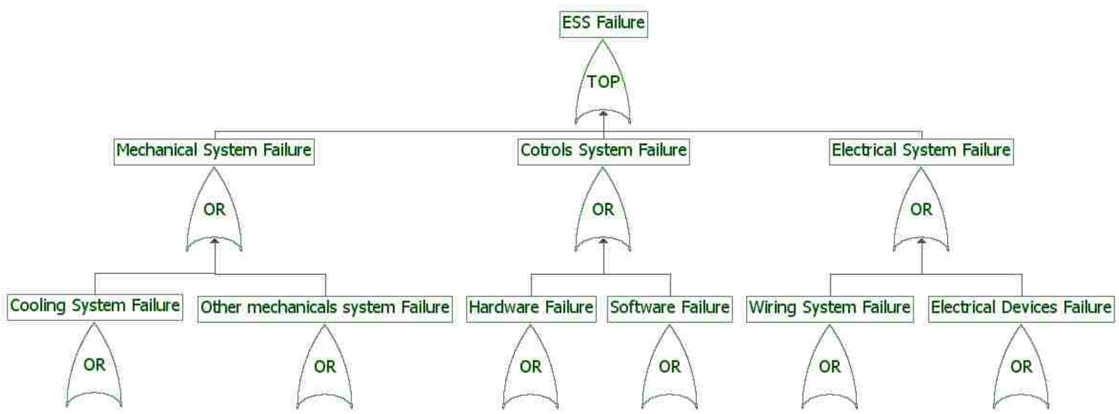

Figure 3.24. FTA for ESS Failure

The six subsystems described above are detailed developed, they are: Cooling System Failure, Other mechanical systems failure, control system hardware failure, control system hardware failure, wiring system failure in the electrical system and electrical components failure. Figure 3.25 presents the structural system failure, in this FTA there are two trigger events that can required the actuation of two subsystems. The first one is extreme structural conditions, i.e. the side or front crash collision that will generate a side acceleration of 20g or a rollover accident which generates an acceleration of 8g upside down. The second trigger accident would be the wrong operation of the ESS modules which will partially o totally produce dangerous gases, this event will required the operation of the venting system, the rupture disc/valve might be the critical component in this scenario. The other sub-systems of failure are described in Figure 3.26-30

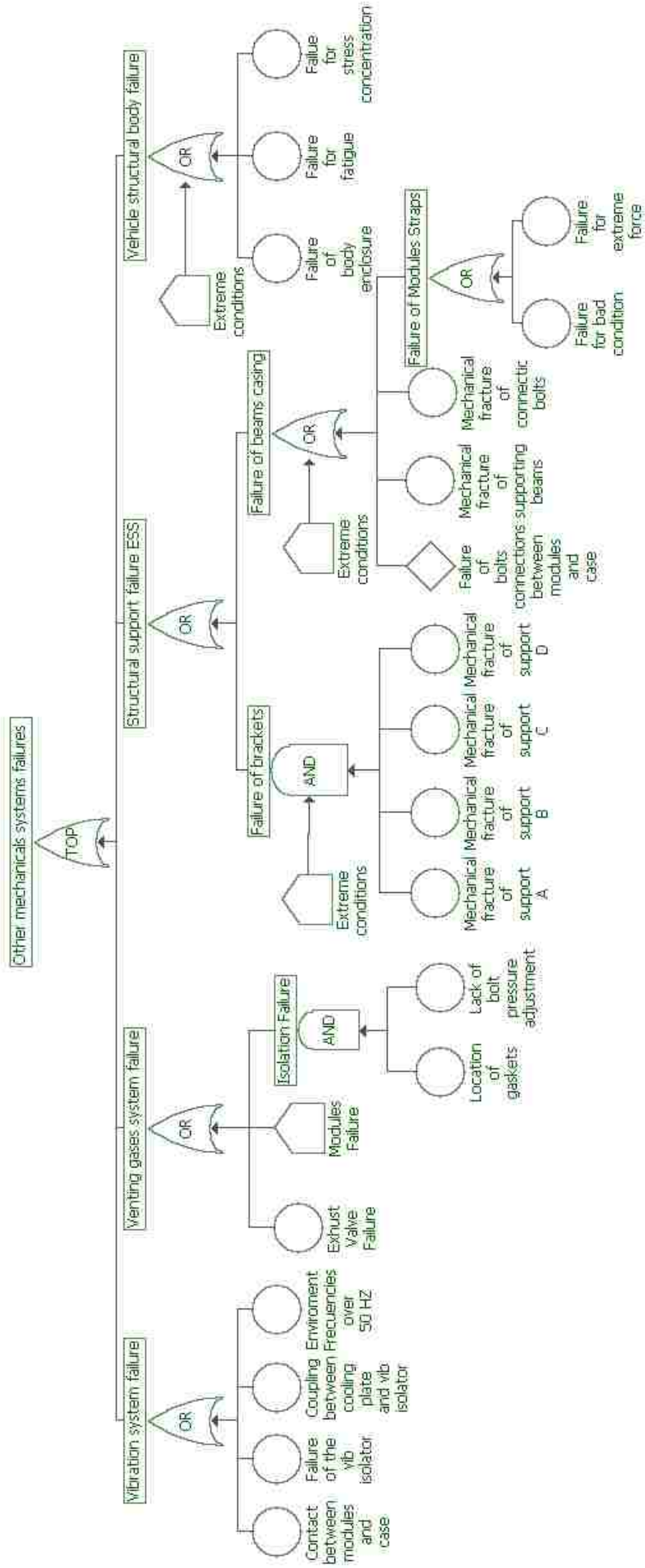

Figure 3.25. FTA for Mechanical Systems Failures

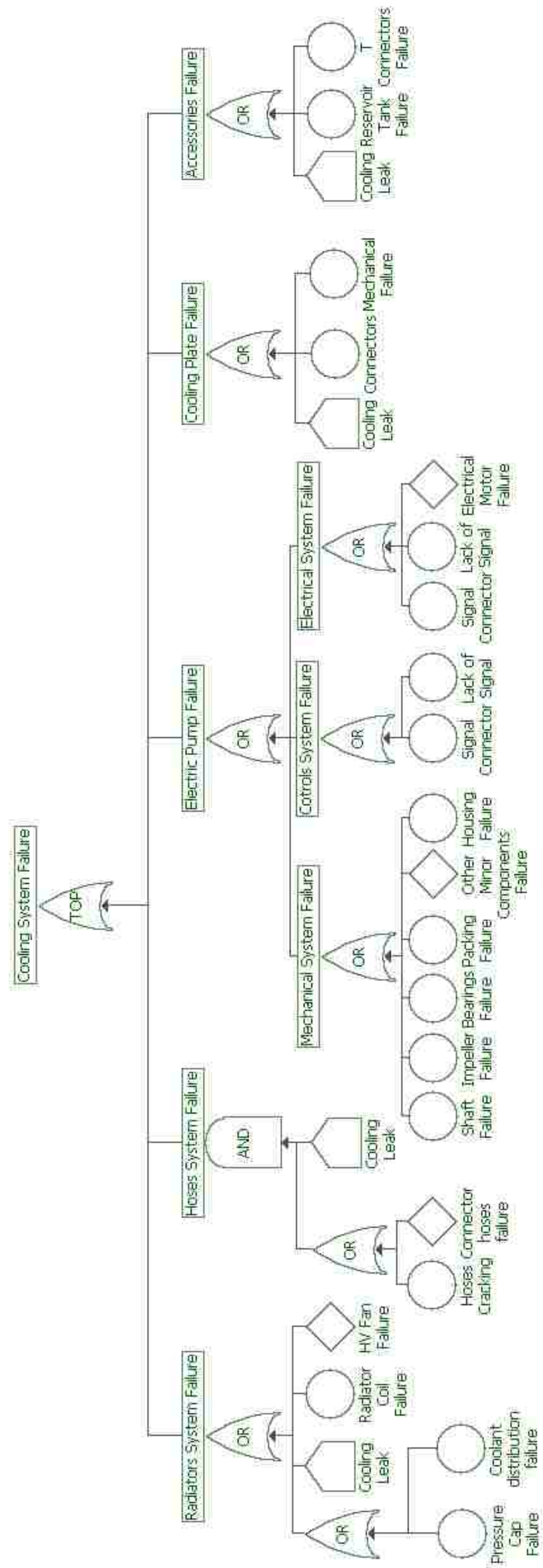

Figure 3.26. FTA for Cooling System Failure

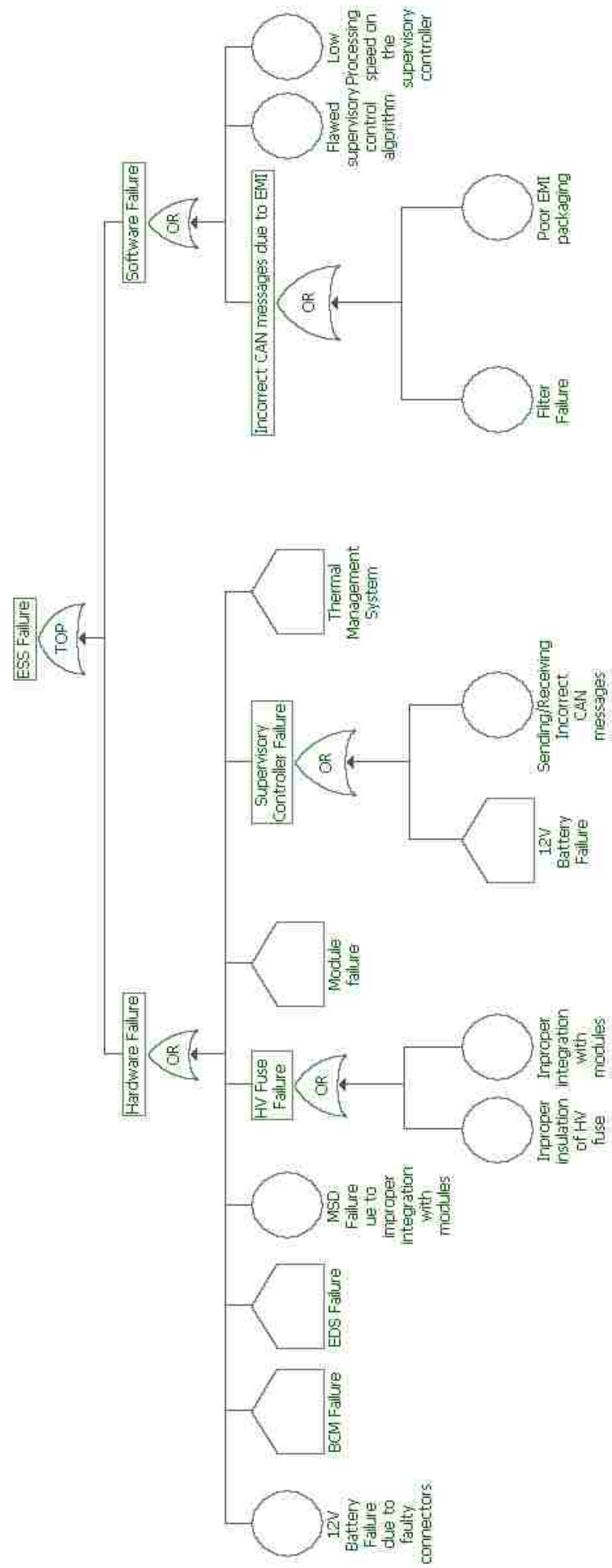

Figure 3.27. FTA for ESS Controls Failure

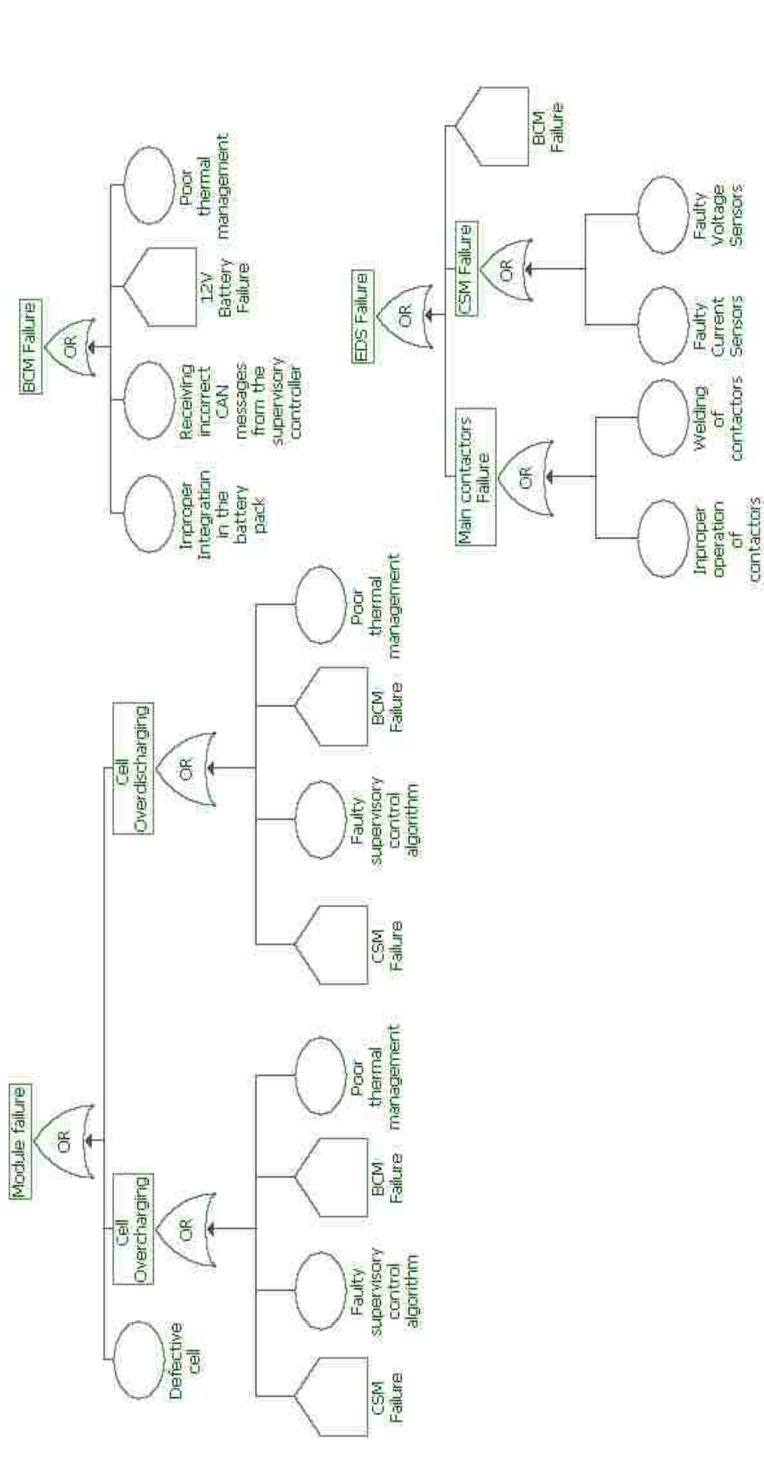

Figure 3.28. FTA for Control Hardware Failure

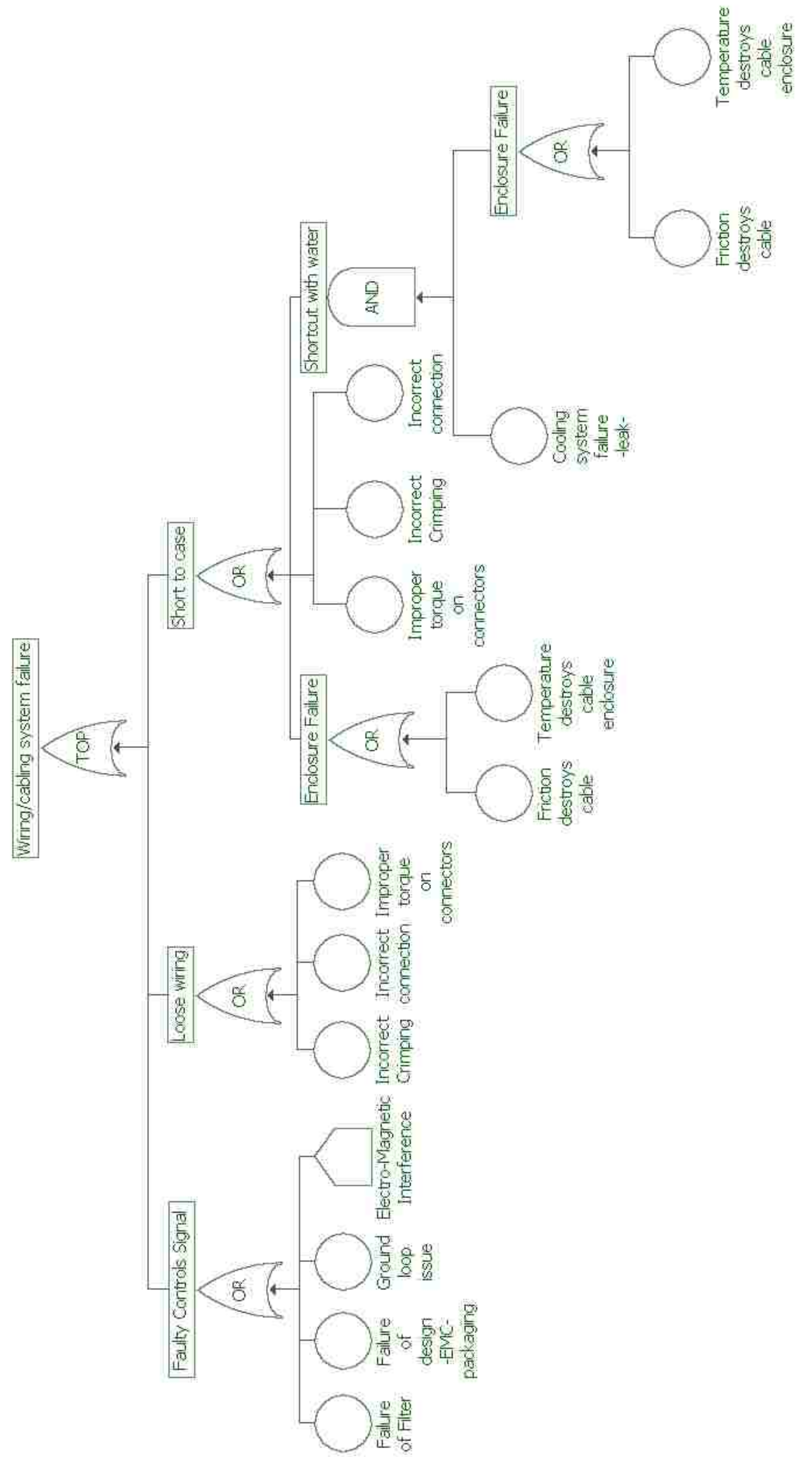

Figure 3.29. FTA for Wiring Failure

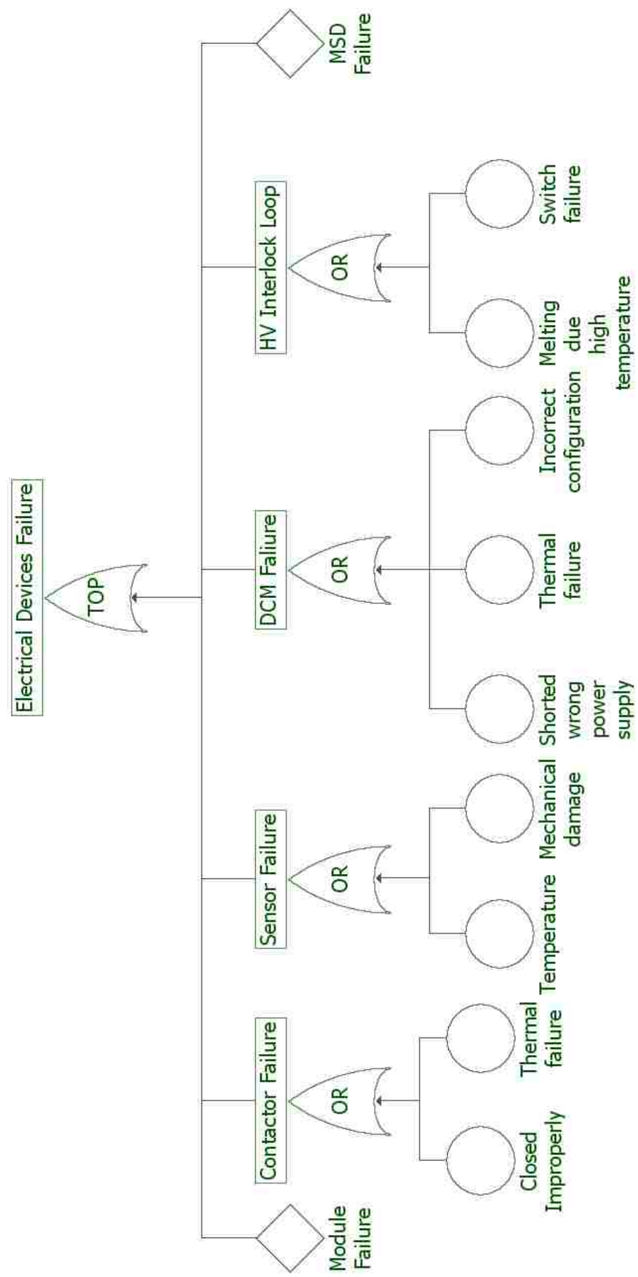

Figure 3.30. FTA for Electrical Devices Failure

There had been indentified 107 basic events between the threes system that may cause the failure of the ESS. The interaction between the controls, electrical and mechanical events are critical for the ESS. It is hard to isolate the events because one non failure event in the mechanical system can cause a failure in the control system.

4. COSTS ANALYSIS

The reason of the present chapter is to illustrate the current costs of developing a high voltage electrical storage system for an extended range vehicle. The main component, which is the lithium ion modules and the corresponding power electronics, has been donated from A123 Systems®.

Moreover, the engineering of developing the cooling system, electrical system and structural analysis is another factor no considered in this document. It took for to the team almost a year to determinate the best location of the ESS in the vehicle and to develop the casing going through several prototypes.

The other main components such as the DC/DC converter and the high voltage charger were bought from BRUSA® accumulating a total cost of $35,000. These include controls software and standard high voltage wiring. The ESS PDM was entirely developed in the electrical area of the Missouri S&T EcoCAR team. The design was perform for the engineering team as well as the electrical senior design team.

In the Mechanical point of view the original design presented in this document was on steel basis with a total cost in material of $2,500 due the weight limit and manufacturability the team decide to develop a second prototype in aluminum with a materials cost of $5,000 the detailed description of material cost are presented in APPENDIXE B. The team received the manufacturing of these components as a donation of Bachman Machine Company. In addition, other minor costs for the case are the hex bolts Grade 12.9 representing $300, vibration isolators $25, nylon straps $60, rupture disc $80, and other minor accessories $100.

The total cost of the battery case was $40,656. This number represents an important opportunity for future manufacturing research to reduce the cost and hence make this technology commercial.

5. CONCLUSIONS AND FUTURE WORK

An entire high voltage pack was develop in Missouri S&T as part of the EcoCAR: The NeXt Challenge competition and it is presented in this document, the design considered several aspects and requirements such as weight, exhaust venting, cooling systems, electrical systems, vibration isolation and structural support. The ESS represents one of the most important components in the develop of the Missouri S&T EcoCAR team Fuel Cell Plug-in Hybrid Electric Vehicle.

The several pathways to produce hydrogen and electricity make the FC-PHEV an ultimate vehicle and it represents a great opportunity of sustainable transportation. These vehicles can run entirely by renewable energies and hence be a ZERO emissions vehicle from Well to the Wheel.

There are several researches on extended range vehicles, some of the main challenges are the cooling systems, battery chemical and increasing the efficiency of power electronics such as inverters and DC/DC converters. Similarly to the PEM Fuel Cell, the cost of manufacturing of this type in mass production represents a great opportunity of future research.

The next step of this prototype is to develop a refrigerant cooling system to cool the batteries in all EV mode, the goal is to increase the temperature difference. Another possibility is to run the cooling system between the cells of the prismatic module to reduce the thermal mass of the modules.

Moreover, the functionality of this ESS would increase if the team is able to remove the air bag sensor to relocate under the ESS and relocate the ESS in a lower position. Add ergonometric to the shape of the battery case to increase the consumer acceptability is an important factor that can be improved in this prototype.

The original design of the ESS was on steel basis, but the team moves to aluminum structure to reduce the weight of the case. The next step of this prototype is to use carbon fiber or composite materials. In a mass production case the carbon fiber option would be the most feasible solution.

The objective of the Fault Tree Analysis is to identify all possible events that might cause a system failure. This analysis can be improved if the probabilities of each components failure are added. The software used for the team allows the user to calculate the final probability of failure and move to a Design Failure Mode Effects Analysis (DFMEA).

The total cost of the ESS is $40,656 however this price does not include the cost of the lithium-ion modules which represents the main cost. The total weight of the system is 322.65 kg which represents an energy/ weight ratio of 46.59 Wh/kg.

APPENDIX A.

RUPTURE DISC FOR EXHAUST SYSTEM

Fike

Data Sheet

AD SERIES - AD, AD-V

DESCRIPTION

The Fike AD Series Bolt Type Rupture Disc is specifically designed for overpressure and/or vacuum protection of atmospheric vessels. The AD-V Series Bolt Type Rupture Discs are designed for overpressure only. For sanitary applications, please see data sheet R.1.44.01 AD-H Series.

FEATURES AND BENEFITS

- Flat disc, no special holders required, install between standard ASME 150 companion flanges. (Other flange ratings available upon request)
- Compressed non-asbestos (Aramid fiber with nitrile rubber binder) gaskets are pre-attached on both sides of disc.
- Standard materials of construction are SST top and bottom sections with Teflon® seal. Other materials are available upon request.
- 50% operating ratio.
- Low burst pressures available, 1 PSIG (.07 BARG) to 15 PSIG (1.034 BARG).
- Standard sizes available 2" (DN50) to 24" (DN600) in nominal pipe sizes. Larger sizes are available.
- Maximum operating temperature is 500°F (260°C)
- Burst in either direction at same pressure (1:1 ratio) **(AD Disc Only)**
- AD-V (Vacuum) bursts in one direction and withstands full vacuum (**Note:** The 24" size will withstand full vacuum from 1-4.50 PSIG (.07-.31 BARG). For pressures greater than 4.50 PSIG (.31 BARG) the AD-V will withstand half vacuum)
- Zero manufacturing range standard

PRESSURE RELIEF VALVE APPLICATION

AD type rupture discs are designed for isolating equipment such as pressure relief valves from corrosive atmospheres. AD discs can be used downstream to protect valve internals and upstream to protect from atmospheric conditions.

ACCESSORIES

AD-BI

- All AD series discs are available with a CSA approved integral burst indicator solution. Specify AD-BI.
- The AD-BI has an 18" lead wire with a weatherproof connector.
- Mating lead cables are available in 10 ft. (P/N D3513-115-10) and 25 ft. (P/N 3513-115-25) lengths

704 S. 10th Street · P.O. Box 610 · Blue Springs, Missouri 64013-0610 U.S.A. · (816) 229-3405 · (816) 229-4615 · www.fike.com

MINIMUM/MAXIMUM BURST PRESSURES IN PSIG (mBARG) @ 72°F (22°C)

		AD, AD-V Discs			
		316/316L SST		Relief Area in² (cm²)	
In	DN	Min. BP	Max. BP	AD	AD-V
2	50	7 (483)	15 (1034)	2.27 (14.60)	1.77 (11.40)
3	80	5 (345)	15 (1034)	5.73 (36.90)	4.52 (29.2)
4	100	4 (276)	15 (1034)	9.62 (62.10)	7.69 (49.6)
6	150	3 (207)	15 (1034)	24.6 (159)	20.59 (133)
8	200	2.5 (172)	15 (1034)	44.2 (285)	38.48 (248)
10	250	2 (138)	13 (896)	70.9 (457)	63.62 (410)
		13.01 (897)	15 (1034)		49.26 (318)
12	300	2 (138)	12 (827)	104 (670)	95.03 (613)
		12.01 (828)	15 (1034)		74.47 (480)
14	350	1.5 (103)	10 (689)	118 (760)	108.43 (700)
		10.01 (690)	15 (1034)		84.49 (545)
16	400	1.25 (86)	9 (620)	159 (1030)	125.90 (812)
		9.01 (621)	15 (1034)		110.96 (716)
18	450	1 (69)	8 (551)	207 (1340)	152.43 (983)
		8.01 (552)	15 (1034)		138.67 (895)
20	500	1 (69)	6 (413)	262 (1690)	181.47 (1171)
		6.01 (414)	15 (1034)		173.96 (1122)
24	600	1 (69)	4.50 (310)	389 (2510)	285.87 (1844)
		4.51 (311)	15 (1034)		254.40 (1641)

* Single or multi-petal designs cannot be selected but are determined by burst pressure and vacuum support. Please consult factory for additional information.

BURST/PERFORMANCE TOLERANCE

- ±1 psig (70 mbarg) on discs 2" (DN50) through 14" (DN350), ± 0.5 psig (35 mbarg) on discs 16" (DN400) and larger.
- ± 1 psig (70 mbarg) when nominal requested pressure exceeds 4 psig (275 mbarg).

GASKET OPTIONS

Gasket Material	Max Temp
Non-Asbestos	500°F (260°C)
Teflon	500°F (260°C)
Viton	450°F (232°C)
Blue Gylon	500°F (260°C)
White Gylon	500°F (260°C)

HOW TO SPECIFY

Previous Lot Number:	
OR	
Size:	
Flange Rating:	
Burst Pressure:	@ (Temperature)
Gasket Material:	
Vacuum:	Yes / No
Integral Burst Indication:	Yes / No
Certification:	CE

Performance Attributes		Process Media		Rupture Disc Holder
Operating Ratio	Vacuum Resistant	Liquid	Vapor / Gas	Companion Flanges
50%	yes*	yes	yes	yes

* Varies by model

CERTIFICATIONS

CE

0036

.

APPENDIX B.

MECHANICAL COMPONENTS FOR THE ESS

Part	Quantity	Dimensions In.	Description	Total Price
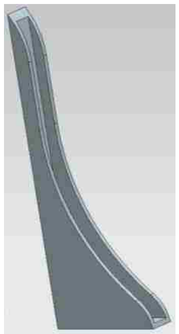	4	8.26” x 2.36” x 25.75” Thickness - 0.38”	4” x 3” x 240” Thickness-3/8” Two steel angles can be placed side by side to get a total of 8 inch. Accordingly the length of 25.7” can be cut apart. This is done both horizontally and vertically. The total 240” can be used for all 4 beams.	$244.80
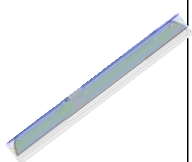	2	2.3” x 1.88” x 51.6” Thickness-0.31”	3” x 2” x 48” Thickness-3/8” Two steel angles can be placed one above the other to get a U shape	$53.04
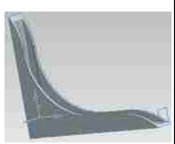	2	18.1” x 13.97” x 2.36” Thickness-0.38”	2” x 2” x 24” Thickness - 3/8” Two angles to be used one in horizontal and another in vertical direction and are welded to get the suitable dimensions.	$42.24
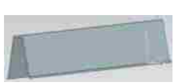	2	3.14” x 3.14” x 31.5” Thickness-0..13”	3” x 2” x 72” Thickness - ¼” Two angles put side by side are welded to get the suitable dimensions.	$30.96

	1	3.14” x 3.14” x 43.7” Thickness- 0..15”	3” x 2” x 48” Thickness - ¼” Two angles put side by side are welded to get the suitable dimensions.	$20.64
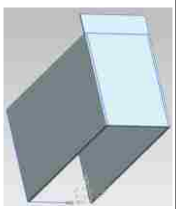	1	8.54” x 19.68” x 11.81”	Two steels plates of dimensions: 12” x 24” x ¼” and 12” x 12” x ¼” are welded.	$52.16
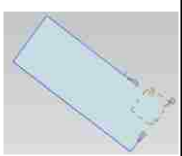	2	25.7” x 10.1” x 0.2”	24” x 12” x ¼”	$62.88
	2	28.74” x 13.07” x 0.2”	24” x 12” x ¼”	$62.88

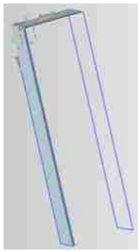	1	46” x 13” x 8”	Two sheets are welded : 48” x 12” x 3/8” and 12” x 12” x 3/16”	$102.36
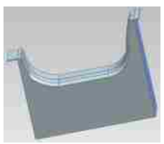	1	750” x 650” x 209”	Three sheets are welded: 48” x 12” x ¼”	$158.64
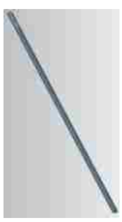	1	45.7” x 0.47” x 0.78”	1-1/2” X ½” X 48” Thickness-1/8”	$10.08
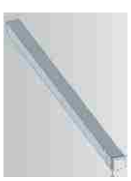	2	2” x 2” x 46” Thickness-¼”	2” x 2” x 48” Thickness-1/4”	$31.36

	2	2” x 2” x 12.63” Thickness-¼”	2” x 2” x 24” Thickness-1/4”	$15.68
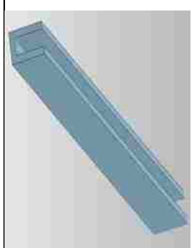	4	25.7” x 0.47” x 0.78”	1-1/2” X 1/2” X 24” Thickness-1/8”	$20.16
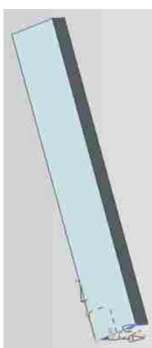	2	45.2” x 7.9” x 2” Thickness-¼”	48” x 12” x ¼” and 12” x 12” x ¼” welded together	$147.20
	2	37.2” x 6.53” x 0.78”	48” X 12” X ¾”	$576.54
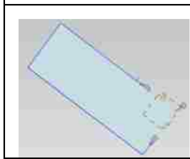	1	13” X 7.9” X 0.35”	12” X 12” X 3/8”	$36.08

	1	1.57" x 1.57" x 7.5" Thickness-¼"	1.5" x 1.5" x 24" Thickness-1/4"	$5.84
	2	29.7" X 0.78" X 0.39" Thickness-2.8"	1-1/2" X ½" X 48" Thickness-1/8"	$10.08
	1	15.74" x 9.8" x 0.19"	24" x 12" x ¼"	$31.44
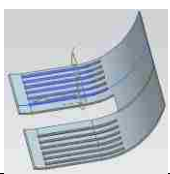	1	46.24" x 35.43" x 0.26"	48" x 48" x ¼"	$114.24
	2	24.54" x 20.27" x 1.06"	24" x 24" x 1"	$530.08
	2	21.45" x 0.46" x 0.35"	1-1/2" x ½" x 48" Thickness-1/8"	$10.08

	2	2” x 2” x 15.35”	2” x 2” x 24” Thickness-1/4”	$7.84
	2	2” x 2” x 21.34”	2” x 2” x 24” Thickness-1/4”	$7.84
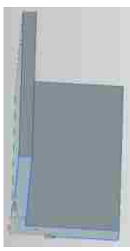	2	1.6” x 1.6” x 7.4”	2” x 2”x 24” Thickness-1/4”	$7.84
	1	16.5” x 8.54” x 0.39”	24” X 12” X 3/8”	$52.16
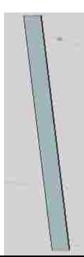	2+2	21.45” x 0.59” x 0.25” and 20.45” x 1.04” x 0.141”	12” x 12” x ¼”	$20.72

BIBLIOGRAPHY

[1] http://www.ecocarchallenge.org/ EcoCAR: The Next Challenge, February 2010.

[2] http://www.eia.doe.gov/oiaf/ieo/world.html U.S. Energy Information Administration: Independent Statistics and Analysis, February 2010.

[3] http://www.eia.doe.gov/aer/pdf/pecss_diagram.pdf Primary Energy Consumption by Sources and Sector 2008, February 2010.

[4] http://en.wikipedia.org/wiki/Oil_price_increases_since_2003 2000s energy crisis, February 2010.

[5] http://en.wikipedia.org/wiki/Greenhouse_gas Greenhouse Gas. February 2010.

[6] Stern, Nicholas 2007. The Economics of Climate Change – The Stern Review Cambridge, UK: Cambridge University Press. February, 2010.

[7] Alley, Richard; et al., "Climate Change 2007: The Physical Science Basis or Policymakers", *10th session of working group I of the IPCC*, 2007.

[8] Yap, David; Reid, Neville; De Brou, Gary; Bloxam, Robert. "Transboundary Air Pollution in Ontario Toronto" *Ontario Ministry of Environment Report 2005.*

[9] bp.com/statisticalreview BP Statistical Review of World Energy June 2009, February 2010.

[10] http://web.mit.edu/mitei/research/spotlights/bandivadekar_thesis_final.pdf Anup P. Bandivadekar "Evaluating the Impact of Advanced Vehicle and Fuel Technologies in U.S. Light-Duty Vehicle Fleet.", February 2010.

[11] BP Statistical Review of World Energy June 2009 http://www.bp.com/liveassets/bp_internet/globalbp/globalbp_uk_english/reports_and_publications/statistical_energy_review_2008/STAGING/local_assets/2009_downloads/statistical_review_of_world_energy_full_report_2009.pdf February 2010.

[12] BP Statistical Review of World Energy June 2009 http://www.bp.com/liveassets/bp_internet/globalbp/globalbp_uk_english/reports_and_publications/statistical_energy_review_2008/STAGING/local_assets/2009_downloads/statistical_review_of_world_energy_full_report_2009.pdf, February 2010.

[13] http://www.ieeeusa.org/policy/positions/PHEV0607.pdf , Position statement plug-vehicles, February 2010.

[14] http://en.wikipedia.org/wiki/Plug-in_hybri Plug-in hybrid, February 2010.

[15] http://www.gmvolt.com/img/upload/2011_chevy_volt_official10_.jpg Chevy Volt, February 2010.

[16] http://image.motortrend.com/f/green/made-in-usa-gm-to-produce-2010-chevrolet-volt-batteries-in-michigan/15564199+w750/2010-chevrolet-volt.jpg Chevy Volt, February 2010.

[17] http://www.gm.com/experience/technology/fuel_cells/fact_sheets/equinox.html Chevrolet Equinox Fuel Cell Spec Sheet, February 2010.

[18] http://i.livescience.com/images/071105-gm-equinox3-02.jpg, LiveSience, February 2010.

[19] Erik Wilhelm, "Model-Based Validation of Fuel Cell Hybrid Vehicle Control Systems Waterloo", Ontario, Canada, 2007.

[20] Toshio Gonai, Takeshi Kiyokawa, Hiroyuki Yamazaki, Masayoshi Goto, "Development of lithium ion battery system for space, report of the result on the result of development of the lithium Ion battery system for space" Kamakura city, Kanagawa, Japan 2003.

[21] Chris Mi, Ben Li , Derrick Buck, and Naoki Ota. "Advanced Electro-Thermal um-ion Battery System for Hybrid Electric Vehicle Application" U.S.A 2007.

[22] http://www.ieahev.org/pdfs/annex_7/annex7_hev_final_rpt_110108.pdf Status Overview of Hybrid and Electric Vehicle technology (2007), February 2010.

[23] http://en.wikipedia.org/wiki/Lithium-ion_battery, Lithium-ion batteries, February 2010.

[24] http://bioage.typepad.com/.a/6a00d8341c4fbe53ef01156ff5a3a8970b-800wi, a123 batteries, February 2010.

[25] http://content.edgar-online.com/edgar_conv_img/2009/09/24/0001047469-09-008512_G692363.JPG , a123 batteries, February 2010.

[26] http://ecocarchallenge.mst.edu , Missouri S&T EcoCAR Team, February 2010.

[27] http://archive.ecocarphoto.com/c/ecocarphoto EcoCAR Pictures, February 2010.

[28] Andrew Meintz, Missouri S& EcoCAR Team, "EcoCAR progress report 4", Rolla Missouri December 2009.

[29] Andrew Meintz, Mehdi Ferdowsi, Kevin B. Martin "Supervisory Control Development of a Fuel Cell Plug-in Hybrid Electric Vehicle" IEEE, Missouri, 2009.

[30] Andrew Meintz, Joseph Ishaku, Edward Anculle, Kevin Martin Missouri S&T EcoCAR Team, "EcoCAR progress report 4", Rolla Missouri December 2009.

[31] http://green.autoblog.com/2006/11/06/gm-selects-quantum-fuel-systems-to-produce-h2-storage-for-equino/ February 2010.

[32] http://www.blogcdn.com/green.autoblog.com/media/2006/11/qtww_tank.png

[33] Technical Session: Crash Safety Hydrogen Fuel Cell Vehicle: Safety & Crashworthiness Mohammed Bahauddin, GM Javeed Mohammed, GM 2005 GM Global CAE Conference, September 12-15, 2005.

[34] http://green.autoblog.com/gallery/general-motors-generation-v-fuel-cell-stack, General Motors Generation V fuel cell stack, February, 2010.

[35] http://www.ecofriendlymag.com/wp-content/plugins/wp-o-matic/cache/32db7_gen1-gen2-fcs-tale-of-tape1-copy.jpg GM Fuel Cell, February 2010.

[36] http://www.ecofriendlymag.com/wp-content/plugins/wp-o matic/cache/32db7_gen1-gen2-fcs-tale-of-tape1-copy.jpg GM Fuel Cell, February 2010.

[37] http://www.technologyreview.com/files/25804/auto_x600.jpg GM Fuel Cell, February 2010.

[38] http://www.brusa.biz/products/e_nlg5112.htm high voltage charger, February 2010.

[39] http://www.brusa.biz/products/e_bdc412347.htm DC/DC converter, February 2010.

[40] http://www.fike.com/products/rdsrl.asp Fike rupture disc, March 2010.

[41] Christopher M. Huston, Murali Bottu, and Mehdi Ferdowsi , "Power Distribution Module Design for the Energy Storage System in Missouri S&T's EcoCAR", November 2009.

VITA

Edward A. Anculle Arauco was born in Arequipa, Peru on June 15, 1984. He is a Mechanical Engineer who grew up in Arequipa, Peru, a small city in the south of Peru where he studied at De La Salle Private School. At 16 years old he was selected to participate in a one-year high school exchange student program in California, U.S.
On May 2007, he received his Bachelor of Science in Mechanical Engineering from the "Pontificia Universidad Catolica del Peru" in Lima, Peru where he was ranked 5th in his class. In order to obtain his Peruvian Engineering Degree he submitted and defended his undergraduate thesis: "5.5 kW hydropower group using a centrifuge pump as a turbine". After working in several companies in Lima, Peru, he began his graduate studies in the Mechanical and Aerospace Engineering Department at Missouri University of Science and Technology, Rolla, Missouri. He serves as the Chief Technology Officer of the Missouri S&T EcoCAR Team and Mechanical Team Leader. He received a Master Degree in Mechanical Engineering on May 2010.